Air Traffic Estimation and Decision Support for Stochastic Flow Management

Prasenjit Sengupta[*], Monish D. Tandale[*], Victor H. L. Cheng[†], and P. K. Menon[‡]
Optimal Synthesis Inc., Los Altos, CA 94022-2777

Development of a decision support system that uses real-time track data to estimate statistical parameters describing the stochastic traffic flow, and then applies modern statistical decision theory to optimize traffic flow is described. An advanced estimation algorithm provides the parameter estimates based on queuing network models of traffic flow. A hypothesis testing approach is developed for triggering traffic flow management initiatives in the terminal area, and a stochastic quadratic programming methodology is advanced to achieve flow control objectives such as runway load balancing. The use of this methodology is demonstrated using multi-day track data from the San Francisco terminal area. It is shown that the methodology can correctly identify the need for restricting the traffic flow into the terminal area, and provide decision support to balance the traffic flow at the runways under uncertain traffic flow conditions. The approach developed in this research can be extended to create decision support tools for a wide variety of stochastic air traffic flow control situations.

I. Introduction

Several research efforts are underway at NASA on air traffic flow management (TFM) using advanced iterative numerical algorithms[1-8]. These algorithms are being considered not only for strategic TFM in the National Airspace System (NAS), but also in managing surface traffic flows. While these algorithms can provide precise solutions to the traffic management problem, they are more suitable for predictive control based on deterministic data. Traffic flow control in the presence of uncertainties inherent in the air traffic management system requires the integration of estimation algorithms to derive the stochastic description of traffic flow, followed by the application Statistical Decision Theory[9] to either trigger iterative numerical algorithms or to create stochastic flow control decisions. The focus of the present research is on stochastic traffic flow control and resource management in the terminal area and the runways.

Under normal circumstances, the aircraft are allowed to operate according to their intent, and no major traffic flow management initiatives are necessary to ensure smooth operation. However, various perturbing influences such as adverse weather require traffic flow management initiatives to be brought into effect to match the available capacity with the demand. The objective of TFM algorithms on the surface as well as in the air is to mitigate the impact of these perturbing factors on traffic flow before they actually become disruptive.

TFM is generally initiated upon the detection of adverse events in the air traffic environment. For instance, low visibility conditions may restrict simultaneous operations on closely-spaced parallel runways. Once adverse traffic flow conditions are predicted to occur, the TFM algorithm can be initiated to mitigate them. Since the predictions are generally based on uncertain data, it is important to rule-out traffic flow restrictions cased by minor flow transients or due to the naturally occurring variability in the traffic. Consequently, decisions to initiate traffic flow management must explicitly recognize the stochastic nature of traffic flow. Since the uncertainties in the system cannot be precisely predicted, the traffic flow parameters must be estimated from actual measurements, followed by the application of methods from Statistical Decision Theory[9] to create actionable decisions.

---

[*] Research Scientist, 95 First Street Suite 240, Senior Member AIAA.
[†] Vice President, 95 First Street Suite 240, Associate Fellow AIAA.
[‡] Chief Scientist and President, 95 First Street Suite 240, Fellow AIAA.

Queuing network models[10-13] can capture the essential stochastic features of traffic flow using three sets of stochastic parameters, namely, the inter-arrival time distribution, service time distribution and the inter-node flow fractions. Because the queuing model parameters are based on aggregated data, and because the queuing network can provide the statistical distributions of the variables of interest, this model is suitable for use as the basis for formulating stochastic estimation algorithms. A recent research effort[14-18] discussed a family of queuing network models suitable for modeling traffic flow in the NAS. It was demonstrated in Ref. 17 that these models can accurately predict the statistics traffic flow, at a fraction of the computational time required for explicit Monte-Carlo simulations.

The stochastic traffic flow parameters derived from the estimation algorithm can be used as the basis for formulating statistical decisions. Two distinct stochastic decision making processes are illustrated in the present work. The first generates triggers for initiating traffic flow management decisions, and the second employs an optimal resource allocation approach to balance the traffic volume between multiple runways.

The TFM triggering algorithm is demonstrated for the San Francisco terminal area, while the resource allocation algorithm is applied to runway load balancing in a specific runway configuration. Actual traffic data[19] from the San Francisco Metroplex comprising the SFO, OAK, and SJC airports is used to demonstrate the performance of these algorithms. As an example, Figure 1 shows the radar tracks of aircraft in the San Francisco (KSFO) terminal area on July 9, 2007. A few trajectories shown in red denote typical vectoring and holding maneuvers in the terminal area to meet arrival time constraints at the runway. The paths marked with bold straight line segments represent the typical waypoint sequence aircraft employ from the boundary of the terminal area to the runway. Note that only the arrival traffic in the *West Plan* is shown in Figure 1.

The overall stochastic flow control concept is illustrated in Figure 2. The first step in the approach is the formulation of the queuing network model of the airspace. As motivated earlier, queuing network captures the essential features of traffic flow using a very small number of parameters. These networks can be used to rapidly compute traffic flow metrics for basing the TFM decisions. Formulation of a queuing network of the San Francisco terminal area will be discussed in Section II. An estimator is next formulated based on the queuing network model. The estimator formulation follows the *Bayesian* approach[20] of using measurements to update *prior* statistical distribution of queuing network parameters. Since the probability distributions employed in queuing networks are non-Gaussian, traditional

Figure 1. Sample Radar Tracks for the *West Plan* Traffic Arrivals into KSFO

estimation techniques such as Kalman Filters[21] cannot be used. However, rapid evolution of computer technology has made it possible to consider more advanced estimation schemes such as the Particle Filtering technique[22,23] for this non-Gaussian estimation problem. The Particle Filtering algorithm used in the present research will be presented in Section III.
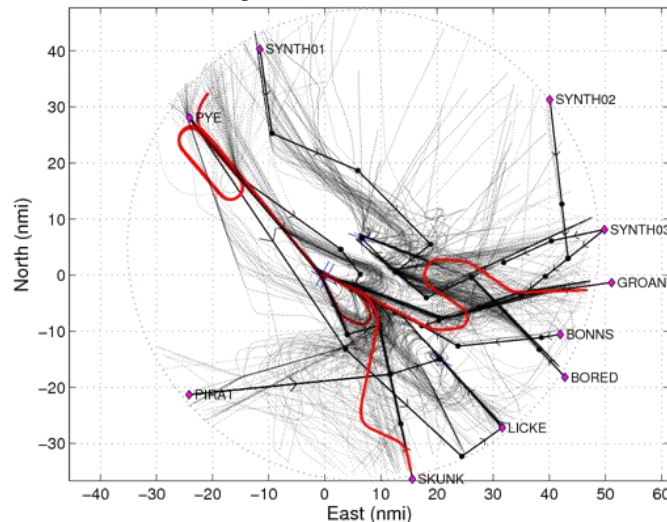

Figure 2. Derivation of Traffic Flow Management Decisions from Stochastic Traffic Data

American Institute of Aeronautics and Astronautics

The estimated queuing parameters can be used to compute the traffic flow metrics to form the basis for air traffic flow management decisions. Common metrics include traffic density in regions of the airspace, flight time between waypoints and traffic flows at specific fixes. The estimation algorithm will enable the computation of statistical distribution of these metrics for use in decision making. Type of decisions to be made in TFM may include the generation of triggers for initiating iterative numerical algorithms, or specific flow control actions such as miles/time-in-trail, holding and vectoring, re-routing and flow balancing. Since the data available is in the form of distributions, these decisions must be formulated using methods from Statistical Decision Theory. Parts IV and V will discuss two different applications of the theory. The first involves the generation of TFM triggers in the San Francisco terminal area based on Hypothesis Testing, and the second involves runway load balancing based on mean traffic flow.

The methodology for traffic flow management advanced in this report explicitly recognizes the stochasticity of the air traffic flow. Consequently, decisions emerging from this methodology are likely to be directly applicable in real situations. Due to its general structure, the stochastic decision making methodology developed in this paper is applicable in a wide variety of traffic management problems. VI will discuss the conclusions from the present research, and will present a few productive avenues for future work.

II. Modeling Traffic Flow in the Terminal Area

As indicated in the previous section, the estimation and decision techniques developed in this research focused on traffic flow control in the San Francisco terminal area. The traffic flows in the San Francisco metroplex according to the *West Plan* are shown in Figure 3. This metroplex includes San Francisco International Airport (SFO), Oakland International Airport (OAK), and Mineta San José International Airport (SJC). The traffic flows into the area under the *South East Plan* is illustrated in Figure 4.
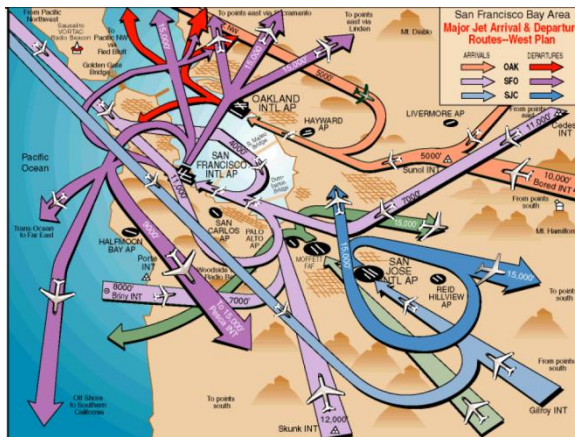

Figure 3. Traffic in the San Francisco Area Metroplex (*West Plan*) Reference[24]
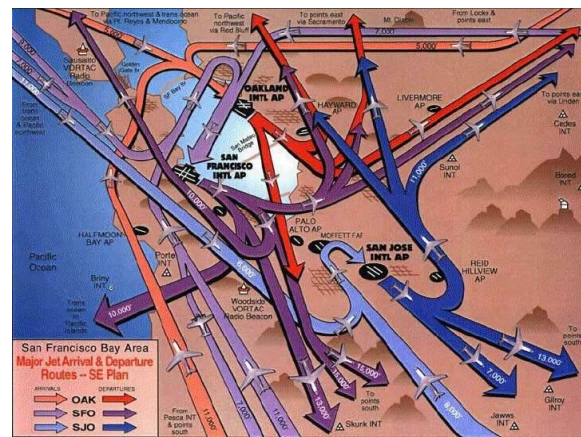

Figure 4. Traffic in the San Francisco Area Metroplex (*South East Plan*) Reference[24]

In the interest of brevity, the development will be restricted to arrivals into the San Francisco metroplex under the West Plan. In the present work, it is assumed that the San Francisco metroplex is composed of 4 runways and 10 arrival fixes. The 4 runways are: KSFO28L, KSFO28R, KOAK29, and KSJC30. Although KSFO also includes runways KSFO01L and KSFO01R, these are used primarily for departing flights under the West Plan. Consequently, these two runways are not included in the present model. Additionally, since the volume of air traffic arriving at KSFO is considerably larger than KOAK or KSJC, the latter two airports are considered to be composed on single runways. Traffic flows under the South East Plan, departure traffic flow, and traffic in and out of the other airports in the metroplex were not analyzed in this research.

A. Modeling the Metroplex as a Network of Arrival Fixes

The trajectories of flights arriving into the metroplex can be modeled as a series of routes between arrival fixes and runways at the airport. The layout of a simplified set of arrival routes for the San Francisco region considered in the present study is given in Figure 5.

The arrival fixes used in the present work are: BORED, BONNS, GROAN, LICKE, PIRAT, PYE, SKUNK, SYNTH01, SYNTH02, and SYNTH03. It can be observed from Figure 5 that all the chosen fixes lie in a circle of

radius approximately 40 nautical miles, with center at KOAK. This is because the radar measurements for flights landing and taking off from the metroplex are only available within this area. The arrival fixes SYNTH01-03 are phantom fixes that are not used in operational procedure, but are used to represent aircraft trajectories from STIKM, SAC, and MODVD, respectively. PIRAT is used to represent flights landing in the metroplex from the Pacific. The other arrival fixes also include waypoints for arrival paths whose arrival fixes lie outside the 40nmi radius. For example, LICKE is a merge point of aircraft trajectories from PAPEE and SNS, and SKUNK represents aircraft trajectories from ANJEE.

Each arrival-fix and runway pair constitutes an arrival route. Even though there are 40 possible combinations of fixes and runways, all fixes do not lead to all runways. With reference to Figure 5, it may be observed that PYE and LICKE are arrival fixes for flights landing at KSJC30, and SYNTH01/03 and BORED are fixes for KOAK. The remainders of the fixes are for flights landing at KSFO. Note that some of the fixes are shared by flights on approach to different airports. For example, a small fraction of Pacific flights routed through PIRAT also land at KSJC. Flights from SYNTH03 land at both KOAK as well as KSFO. The radar measurements indicate that there are typically 18 active fix-runway combinations. The exact number may change from one day to next, depending on the flight schedules.
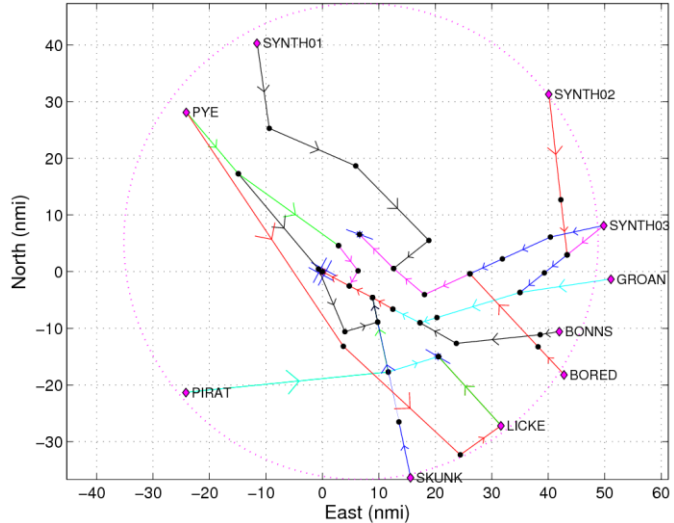

Figure 5. Arrival Fixes in the San Francisco Metroplex

B. Abstraction of Arrival Routes as a Queuing Network System

The queuing abstraction[10,11] of an air-route models the aggregate behavior traffic using two parameters, namely, the *Inter-Arrival Time* distribution into the arrival fix and a *Service Time* distribution through the route. Since the service time is not deterministic, the model denotes delayed traffic as a queue of aircraft waiting to complete their flight through the route. Figure 6 illustrates a typical queuing model. The red circle represents the service time or the time of flight through the route, given by a statistical distribution. For instance, individual aircraft take a certain amount of time to transit between waypoints. A certain amount of variability will exist due to ambient winds and aircraft type. The second component of the queue depends upon the arrivals into the queuing node. Depending on the traffic existing between the waypoints of interest, the aircraft entering the route segment may have to extend its flight time to follow the aircraft already en route. This additional flight time can be interpreted as the *Wait Time* spent in a queue, represented blue a blue-red accordion in Figure 6. Since the wait time cannot be explicitly separated out, it is more convenient to conceptualize the total time spent in a route as the *System Time*. Note that the system time can directly be measured along each route by subtracting the time of entry of each aircraft into the route from the time of exit from the route segment. Discussions in Section III will demonstrate how estimation can be used to construct the system time distribution from prior knowledge about the route and actual measurements.

Admittedly, as with the Eulerian model of traffic flow, a certain amount of fidelity in traffic representation is lost due to the fact that the queuing abstraction condenses the aggregate behavior of the aircraft in the airspace through service time and wait time in the queue. The chief justification for their continued use in applications stems from the fact that they enable extremely rapid stochastic analysis of traffic flows using simple algebraic relationships.
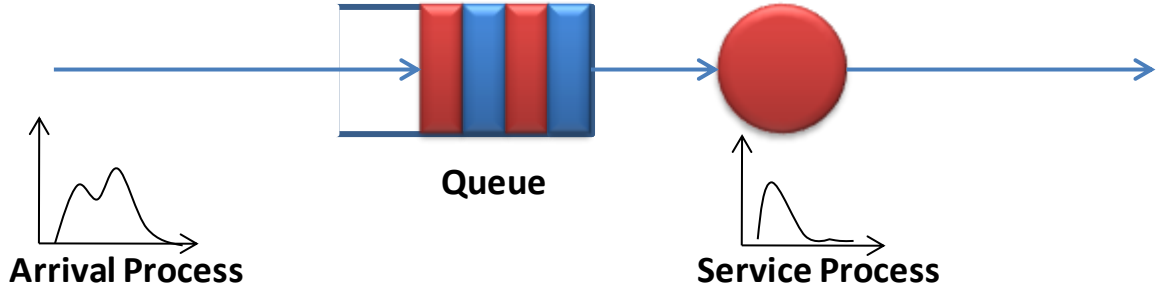
American Institute of Aeronautics and Astronautics

Figure 6. Queuing System with an Arrival Process, Queue and a Service Process

The traffic flow in the NAS will generally involve multiple route segments that merge and diverge. The traffic along these routes can be represented using a queuing network composed of several queues. If the network contains diverging nodes, additional parameters called *Flow Fraction*[10] will also have to be defined. As an example, Figure 7 shows the queuing network abstraction of the traffic arriving into the San Francisco airport. It may be noted that this network consists only of merging nodes. The estimation methodology described in Section III enables the computation of the queuing network by combining historic data, with current measurements, in a predictor-corrector type algorithm.
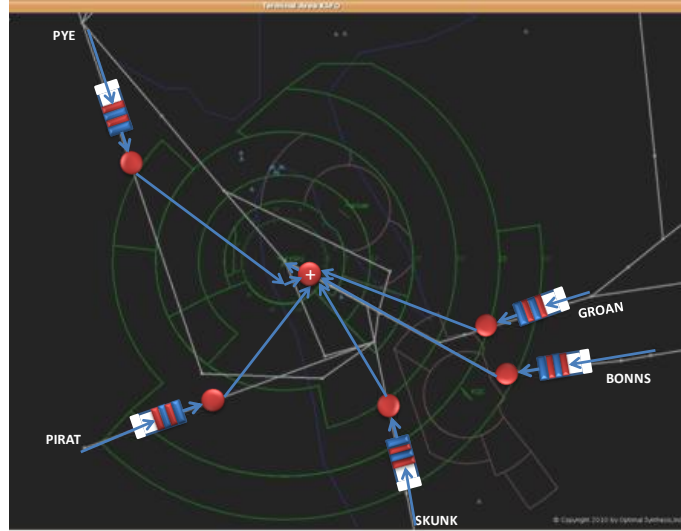

Figure 7. Queuing Network Approximation of the San Francisco Terminal Area Traffic

III. Particle Filter for Estimating Air Traffic Flow Queuing Network Parameters

The statistical distribution of queuing network parameters for traffic flow discussed in Section II can be determined from historic traffic data. However, since the traffic data is available continuously, an approach must be found to update the parameter distributions derived from historic data to detect changes. This can be carried out using the Bayesian approach[20,21]. This parameter estimation approach uses the Bayes theorem to update *prior* statistical distributions using *evidence* in the form of measurements to get *posterior* or updated distributions. A well-known implementation of this approach is the Kalman Filter[21], and related estimation techniques. The Kalman Filtering approach is a specialization of the Bayes estimation technique to linear dynamic systems with Gaussian noise components to derive recursive algebraic relationships for deriving posterior distributions from prior distributions and measurements. Due to its elegance and computational efficiency, the Kalman Filtering technique has found applications in extremely diverse set of problems.

Unfortunately, the Kalman Filter approach cannot be employed in estimating the parameters of the queuing network because of two reasons. Firstly, the inter-arrival time distributions, service time distributions and the flow fractions are all constrained to be greater than zero. Secondly, these distributions are described by Poisson, Erlang or Coxian distributions[10,11]. These facts require the consideration of more advanced techniques such as Particle Filtering algorithms[20,22,23]. An overview of the Particle Filter and its application to the estimation of queuing network parameters will be discussed in this section.

Model describing the parameters of the queuing network can be represented as:

$$x_{k+1} = f(x_k, v_k)$$
$$z_k = h(x_k, \mu_k)$$

(1)

In the above equation, x_k is the state of the model at the kth instant, z_k is the measurement, ν_k is the process uncertainty in the nonlinear transformation $f: \mathbb{R} \to \mathbb{R}$, and μ_k is the measurement uncertainty for the measurement model $h: \mathbb{R} \to \mathbb{R}$. To avoid complicated subscripts, it is assumed that the nonlinear system and the measurement models are scalar. However, the analysis presented in this section holds for multi-dimensional systems as well.

In the present work, Eq. (1) describes the evolution of the *System Time* estimate at a given arrival fix-runway route, with measurements available from radar measurements. In the absence of any process uncertainty, the estimate of the System Time will remain unchanged, and $\hat{x}_{k+1} = \hat{x}_k$, where the $\hat{}$ superscript denotes the estimated value of the quantity. However, in general, uncertainty in the process arises due System Time variation caused by factors such as the aircraft fleet mix, prevailing wind pattern, weight variations, piloting technique, among others.
In the absence of measurement uncertainty, $\tilde{z}_k = \tilde{x}_k$, where the $\tilde{}$ superscript denotes the measured value of the quantity. However, measurement uncertainty will be present due various factors affecting radar estimation of aircraft positions.

The particle filter is used to represent the distribution of the state at the kth step, by a set of particles $X = \{\hat{x}_k^i\}$, $i = 1, \dots, N$, where N is the number of particles. As a general rule, a larger number of particles will result in a more accurate representation of the probability density function (PDF) of $\hat{x}_k$. To complete the description of the PDF, it is also necessary to use a set of *importance weights* $\Omega = \{w_k^i\}$, $i = 1, \dots, N$. At the kth step, the weight w_k^i denotes the relative weight of the particle $\hat{x}_k^i$ in the representation of the PDF. Consequently, the posterior distribution $p(x_k|z_0, z_1, \dots, z_k)$ is approximated by the N-tuple set $P = \{(\hat{x}_k^1, w_k^1), (\hat{x}_k^2, w_k^2), \dots, (\hat{x}_k^N, w_k^N)\}$. An approximation for the expected value of a function $g(x_k)$ is then given by:

$$\int g(x_k)p(x_k|z_0, z_1, \dots, z_k)dx_k \approx \sum_{i=1}^{N} w_k^i g(\hat{x}_k^i) \tag{2}$$

A. Process and Measurement Uncertainty Models

The process noise model can be given in terms of a known PDF. For instance, if the noise component were Gaussian, the distribution can be specified in terms of mean and variance. In the most general case the process and measurement noise uncertainties can be given by histograms or discrete PDFs derived from historic or experimental data. If the process uncertainty is given by a discrete PDF, Eq. (1) can be rewritten as:

$$x_{k+1} = f(x_k, p_{k_1}, p_{k_2}, \dots, p_{k_n}) \tag{3}$$

where $(p_{k_1}, \dots, p_{k_n})$ denote the histogram heights proportional to frequency, over time interval sets $T_i = [t_0, t_i)$, with $t_0 < t_1 < \cdots < t_i < \cdots < t_n$. The subscript k is used to denote their value at the kth step. Note that T_i are considered constant. The PDF for the measurement uncertainty can also be obtained in a similar manner:

$$z_k = h(x_k, q_{k_1}, q_{k_2}, \dots, q_{k_m}) \tag{4}$$

where the histogram depicting the measurement noise characteristics are defined by m bins of height $q_{k_1}(x_k), q_{k_2}(x_k), \dots q_{k_m}(x_k)$, over time segments T_i' that can be assumed to be constant.

In order to expedite the random number generation required for Particle Filter, this work uses the Gamma (Γ) distribution to model the process and measurement uncertainty. The Γ distribution has a support $[0, \infty)$ and is defined using two parameters k and θ, as follows:

$$p(t) = \frac{1}{\Gamma(k)} \frac{t^{k-1}}{\theta^k} \exp\left(-\frac{t}{\theta}\right) \tag{5}$$

The two parameters can be obtained in terms of the mean m and variance v of the distribution, by using the relations $k\theta = m$, and $k\theta^2 = v$. The Γ distribution is used for the following reasons:

- For integer values of k, the Γ distribution is a k-stage Erlang distribution with rate parameter θ. Physically, this means that a flight that arrives at a fix will go through k phases, each phase will require an amount of time whose value is sampled from an Exponential distribution with mean flow rate $1/\theta$. This type of distribution is commonly used in formulating queuing networks.

- The domain for the Γ distribution is defined as $[0, \infty)$, the random numbers generated by this distribution is guaranteed to be greater than or equal to zero.
- The generation of random variables from a Γ variate is easier when compared to the generation using a histogram. The present research used the GNU Scientific Library[25] routine GSL_RAN_GAMMA[26] for this purpose.

B. The Particle Filter Algorithm

In this paper, the Particle Filtering algorithm is used for the estimation of the System Times along the multiple arrival routes into San Francisco. The steps in the algorithm update this distribution based on a measurement and process model. The steps are as follows:

1. Initialize the distribution of the queuing network parameters using historic data and predicted traffic demand.
2. Generate predictions of the measurements corresponding to the queuing network parameters. Measurement noise and any nonlinear relationship between the queuing network parameters and actual measurements can be included in this step.
3. Update Importance Weights from predictions of measurements and the corresponding queuing network parameters. Importance Weights denote the relative contribution of each particle to the overall statistical distribution.
4. Calculate stochastic distribution of the parameters from the Importance Weights.
5. Carryout Importance Resampling. This step refocuses the set of samples to the regions in the state space with high posterior probability[20,22,23].
6. Use the stochastic distribution of parameters obtained in Step 4 to predict the parameter distributions in the next time step. This prediction can incorporate the knowledge of uncertainties in the queuing network modeling of traffic flows.
7. Go to Step 2, repeat until the estimation process is complete or all measurements have been made.

In the interests of brevity, only a brief description of the Particle Filter in the context of the current application, is presented. Reference 20 provides a thorough discussion of the algorithm. The block diagram given in Figure 8 illustrates the methodology for System Time estimation.
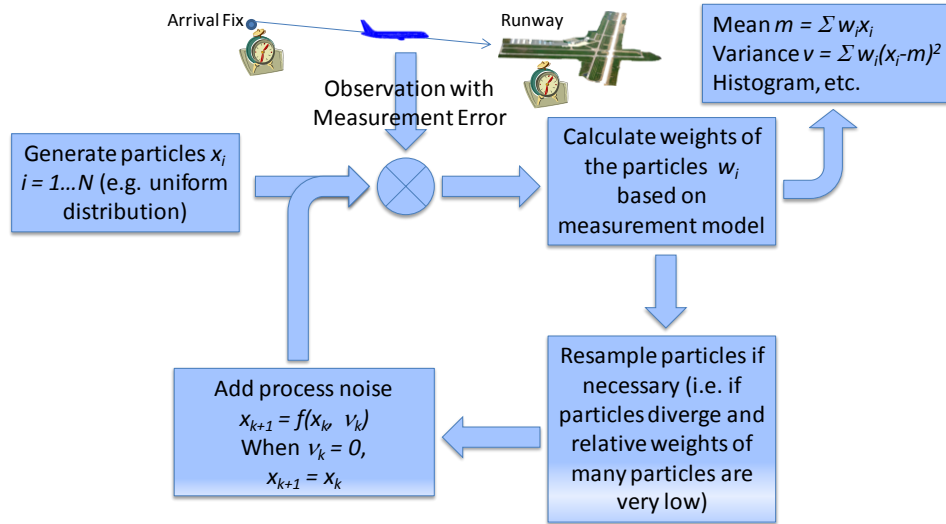

Figure 8. Particle Filter for Estimating *System Time* along an Arrival Route

It is assumed that N particles are used represent the System Time distribution in the Particle Filter. These particles are denoted by $\hat{x}_k^i$, $i = 1, \ldots, N$. It should be noted that $k = 0$ when initialized. The particles can be initialized by sampling $\hat{x}_k^i$ from either a Uniform distribution, or from the histogram described by $(p_{0_1}, p_{0_2}, \cdots, p_{0_n})$ defined in Eq. (3).

Next, the observations corresponding to the particles are generated using the measurement model $z_k = h(x_k)$. Since the measurement is the state System Time,

$$\hat{z}_k^i = \hat{x}_k^i, \; i = 1, \ldots, N \qquad (6)$$

The importance weight w_k^i denotes the relative contribution of the ith particle to the histogram of the state at the kth step. All the stochastic properties of the state x_k are given by a combination of the particles and their weights. Once the measurement $\tilde{z}_k$ is available at the current time, the weight ω_k^i for the ith particle can be calculated as

$$w_k^i = w_{k-1}^i \, p\!\left(\tilde{z}_k | \hat{x}_k^i\right), \; i = 1, \ldots, N \qquad (7)$$

Equation (7) shows that the ith particle weight is the probability that the particle generates the observed measurement, weighted with its value at the previous step. Without loss of generality, one may use $w_0^i = 1$, $i = 1, \ldots, N$. In this work, it is assumed that the observation model is given by a Γ distribution. Consequently, the observation PDF can be constructed using the particle $\hat{x}_k^i$ as the mean, and with a standard deviation σ_R, that is assumed known from prior experiments. For example, the accuracy of radar measurements is known *a priori*. In this case, using Eq. (5) with Eq. (7) results in the following expression for the importance weights:

$$w_k^i = \frac{w_{k-1}^i}{\Gamma(a)} \frac{(\tilde{z}_k)^{a-1}}{b^a} \exp\!\left(-\frac{\tilde{z}_k}{b}\right) + \epsilon, i = 1, \ldots, N$$
$$b = \frac{\sigma_R^2}{\hat{x}_k^i}, a = \frac{\hat{x}_k^i}{b} \qquad (8)$$

In the above equation, a small number ϵ (10^{-8}) is added to the importance weight to prevent it from going to zero due to rounding errors during the evaluation of the Γ distribution PDF through the exponentiation operation and calculation of the gamma functions. Finally, due to rounding and floating point errors, the weights are also normalized with respect to their sum, to ensure that they add to unity.

Given the particles and their weights, a PDF of the state estimate $\hat{x}_k$ can be constructed[20]. In particular, the mean and the variance of the state estimate at the kth step are given by:

$$E[\hat{x}_k] = \sum_{i=1}^{N} w_k^i \hat{x}_k^i$$
$$V[\hat{x}_k] = \sum_{i=1}^{N} w_k^i \left(\hat{x}_k^i - E[\hat{x}_k]\right)^2 \qquad (9)$$

Finally, the system is propagated using the dynamical system equations in Eq. (3). Each particle $\hat{x}_k^i$ is propagated forward using the transformation *without the uncertainty model*, yielding the state $\hat{x}_{k+1}^{i-}$. In the present work, the System Time does not change after an iteration if there is no process uncertainty, i.e., $\hat{x}_{k+1}^{i-} = \hat{x}_k^i$, $i = 1, \ldots, N$. Therefore, the propagated particle can be obtained by sampling from a discrete PDF using the particle at the kth step:

$$\hat{x}_{k+1}^i \sim Hist\left(p_{k_1}(\hat{x}_k^i), p_{k_2}(\hat{x}_k^i), \ldots, p_{k_n}(\hat{x}_k^i)\right), \qquad i = 1, \ldots, N \qquad (10)$$

In this work, it is assumed that the process uncertainty is Γ distributed, i.e. the System Time distribution can be represented by a Γ distribution. Equation (10) can be used to simplify the forward update equation as:

$$\hat{x}_{k+1}^i \sim \Gamma(a, b) \; i = 1, \ldots, N$$
$$b = \frac{\sigma_Q^2}{\hat{x}_k^i}, a = \frac{\hat{x}_k^i}{b} \qquad (11)$$

where σ_Q is the standard deviation of the process uncertainty, determined from traffic data for a normal day with minimal air traffic delays.

With particles propagated as described in the foregoing, the particle filtering procedure is repeated by iterating through the above step until all measurements are accounted for. Under the assumption that both process and measurement uncertainties are distributed according to the Γ distribution, the quantities σ_R in Eq. (8) and σ_Q in Eq. (11) can be considered as the tuning parameters governing the performance of the filter.

C. Estimation of KSFO Traffic Parameters using the Particle Filter

In this section, the Particle Filter algorithm will be used to estimate System Time distributions from radar measurements. The schematic diagram in Figure 8 explains this process. The measurement is the System Time of an aircraft corresponding to the time an aircraft spends along an arrival route. This is obtained from radar measurements that records the time at which a given aircraft is closest to an arrival fix, and the time at which the aircraft lands on one of the runways.

Data for two different days are chosen to illustrate the ability of the estimation scheme to adapt to varying traffic conditions. The first day, July 9, 2007, was a normal day in which air traffic arrivals into San Francisco experienced no constraints or delays as shown in a reproduction of the ASPM data[27] in Figure 9. However, the ASPM data shows that on July 16, 2007, San Francisco experienced a significant drop in capacity during the day. This data is given in Figure 10.

Figure 9 and Figure 10 correspond to Monday, and as such, it is expected that the traffic pattern on both days would closely resemble each other. It may observed from the fight-most column in Figure 9 that there was no impact from weather. A normal variation in total runway capacity can be observed in the 9th column at 10am, followed by a dip in capacity at 10pm. The capacity in this column is represented by the number of runway operations per hour, and is composed of aircraft that are either taking off / departing from the airport, and landing / arriving at the airport.

Airport	Sched Dep Date	Local Hour	Sch Dep	Sch Arr	Act Dep	Act Arr	Act Tot	ADR+ Cap AAR	Runway Conf (Arr|Dep)	Wx Cond	Avg Taxi Out Tm	Avg Taxi In Tm	Temp (F)	Wind Dir	Wind Spd (Knots)	Ceiling (100ft)	Vsby (Stat Miles)	Arpt Wx	Weather Impact
SFO	07/9/2007	0	6	5	6	8	14	72	28L, 28R | 1L, 1R	VAC	14.33	4.67	57	280	6		10.00		None
SFO	07/9/2007	1	6	2	8	3	11	72	28L, 28R | 1L, 1R	VAC	14.50	4.00	57	270	6		10.00		None
SFO	07/9/2007	2	1	1	2	2	4	72	28L, 28R | 1L, 1R	VAC	12.00	0.00	57	290	7		10.00		None
SFO	07/9/2007	3	0	0	0	0	0	72	28L, 28R | 1L, 1R	VAC	0.00	0.00	56	250	5		10.00		None
SFO	07/9/2007	4	0	0	0	2	2	72	28L, 28R | 1L, 1R	IAC	0.00	0.00	57	240	5	012	10.00		None
SFO	07/9/2007	5	0	7	0	7	7	72	28L, 28R | 1L, 1R	IAC	0.00	5.14	57		5	012	10.00		None
SFO	07/9/2007	6	26	7	24	5	29	72	28L, 28R | 1L, 1R	IAC	17.70	4.43	57	280	6	012	10.00		None
SFO	07/9/2007	7	31	17	30	22	52	72	28L, 28R | 1L, 1R	IAC	14.25	4.32	58	000	0	012	10.00		None
SFO	07/9/2007	8	35	30	35	27	62	72	28L, 28R | 1L, 1R	IAC	15.70	5.30	61	160	6	012	10.00		None
SFO	07/9/2007	9	32	34	33	30	63	72	28L, 28R | 1L, 1R	VAC	19.25	4.78	63	050	3		10.00		None
SFO	07/9/2007	10	31	34	20	38	58	107	28L, 28R | 1L, 1R	VAC	18.15	6.06	66	020	8		9.00		None
SFO	07/9/2007	11	31	37	34	53	87	110	28L, 28R | 1L, 1R	VAC	18.59	8.15	66	020	8		9.00		None
SFO	07/9/2007	12	42	29	43	35	78	110	28L, 28R | 1L, 1R	VAC	25.89	7.53	68	020	7		10.00		None
SFO	07/9/2007	13	33	27	41	37	78	110	28L, 28R | 1L, 1R	VAC	25.94	8.60	70	VR	3		10.00		None
SFO	07/9/2007	14	24	27	40	32	72	110	28L, 28R | 1L, 1R	VAC	17.92	5.41	70	240	10		10.00		None
SFO	07/9/2007	15	27	25	32	24	56	110	28L, 28R | 1L, 1R	VAC	16.86	4.30	71	220	6		10.00		None
SFO	07/9/2007	16	23	23	38	34	72	110	28L, 28R | 1L, 1R	VAC	15.04	5.00	71	VR	6		10.00		None
SFO	07/9/2007	17	20	33	24	28	52	110	28L, 28R | 1L, 1R	VAC	15.67	4.76	69	190	9		10.00		None
SFO	07/9/2007	18	28	21	27	30	57	110	28L, 28R | 1L, 1R	VAC	15.43	6.52	65	240	9		10.00		None
SFO	07/9/2007	19	20	33	29	30	59	110	28L, 28R | 1L, 1R	VAC	16.43	5.52	64	240	9		10.00		None
SFO	07/9/2007	20	23	32	22	33	55	108	28L, 28R | 1L, 1R	VAC	16.96	6.45	62	230	7		10.00		None
SFO	07/9/2007	21	14	39	17	35	52	102	28L, 28R | 1L, 1R	VAC	16.67	5.74	61	000	0		10.00		None
SFO	07/9/2007	22	30	17	26	22	48	72	28L, 28R | 1L, 1R	VAC	21.47	13.17	60	290	6		10.00		None
SFO	07/9/2007	23	13	15	18	19	37	72	28L, 28R | 1L, 1R	VAC	17.00	6.00	59	290	6		10.00		None

Figure 9. ASPM Data for Runway Operations at KSFO, July 9 2007

On the other hand, the Data for July 16, given in Figure 10 shows that runway capacity only increased after 12 pm, and decreased after 7 pm. Moreover, the 19th column reveals that the cause for this decrease was fog in the vicinity of the airport as denoted by the notation VCFG. Consequently, it may be expected that the System Time estimates from radar track data on these two days will also exhibit these variations.

The figures given in the following illustrate System Time estimates for arrival into KOAK29, KSJC30, and KSFO28L/KSFO28R. The ASPM data reveals that the decrease in airport capacity was not evident at KOAK and KSJC. However, arrival routes to these airports may still exhibit a deviation in System Time from their calculated nominal values given in Table 1. Although the System Time can be calculated for any route, results are presented only for arrival routes that have a significant number of flights given in Figure 11 through Figure 20.

Airport	Sched Dep Date	Local Hour	Sch Dep	Sch Arr	Act Dep	Act Arr	Act Tot	ADR+ Cap AAR	Runway Conf (Arr|Dep)	Wx Cond	Avg Taxi Out Tm	Avg Taxi In Tm	Temp (F)	Wind Dir	Wind Spd (Knots)	Ceiling (100ft)	Vsby (Stat Miles)	Arpt Wx	Weather Impact
SFO	07/16/2007	0	6	5	11	5	16	72	28L, 28R | 1L, 1R	IAC	13.50	5.33	58	270	14	008	9.00		None
SFO	07/16/2007	1	6	2	8	4	12	72	28L, 28R | 1L, 1R	IAC	14.67	5.50	58	270	14	008	9.00		None
SFO	07/16/2007	2	1	1	1	0	1	72	28L, 28R | 1L, 1R	IAC	12.00	0.00	58	260	10	005	9.00		None
SFO	07/16/2007	3	0	0	0	0	0	72	28L, 28R | 1L, 1R	IAC	0.00	0.00	58	260	10	005	9.00		None
SFO	07/16/2007	4	0	0	0	0	0	72	28L, 28R | 1L, 1R	IAC	0.00	0.00	58	260	11	005	10.00		None
SFO	07/16/2007	5	0	7	0	9	9	72	28L, 28R | 1L, 1R	IAC	0.00	3.75	59	270	14	009	10.00		None
SFO	07/16/2007	6	26	7	24	7	31	72	28L, 28R | 1L, 1R	IAC	15.58	4.71	58	260	16	009	10.00		None
SFO	07/16/2007	7	30	17	29	21	50	72	28L, 28R | 1L, 1R	IAC	14.13	5.47	58	260	24	005	8.00		None
SFO	07/16/2007	8	35	28	31	28	59	72	28L, 28R | 1L, 1R	IAC	20.06	6.48	58	260	24	005	8.00		None
SFO	07/16/2007	9	31	35	29	25	54	68	28L, 28R | 28L, 28R	IAC	26.32	5.82	60	270	18	005	10.00		None
SFO	07/16/2007	10	31	33	26	25	51	72	28L, 28R | 28L, 28R	IAC	18.03	6.30	62	270	15	012	10.00		None
SFO	07/16/2007	11	31	38	28	38	66	98	28L, 28R | 1L, 1R	IAC	18.34	6.33	63	280	15	014	10.00		None
SFO	07/16/2007	12	40	28	39	47	86	110	28L, 28R | 1L, 1R	VAC	20.83	8.79	65	290	15		10.00		None
SFO	07/16/2007	13	34	28	43	29	72	110	28L, 28R | 1L, 1R	VAC	19.53	10.76	66	260	20		10.00		None
SFO	07/16/2007	14	25	26	35	24	59	110	28L, 28R | 1L, 1R	VAC	16.04	6.88	66	260	20		10.00		None
SFO	07/16/2007	15	26	24	22	33	55	110	28L, 28R | 1L, 1R	VAC	15.18	7.88	65	270	18		10.00		None
SFO	07/16/2007	16	23	24	38	27	65	110	28L, 28R | 1L, 1R	VAC	15.43	4.69	64	260	18		10.00		None
SFO	07/16/2007	17	19	32	27	29	56	110	28L, 28R | 1L, 1R	VAC	15.32	4.97	64	290	17		10.00		None
SFO	07/16/2007	18	28	20	29	29	58	110	28L, 28R | 1L, 1R	IAC	16.97	5.86	60	260	14	012	7.00	VCFG	Severe
SFO	07/16/2007	19	20	33	26	23	49	72	28L, 28R | 1L, 1R	IAC	15.00	4.71	60	270	10	010	7.00	VCFG	Severe
SFO	07/16/2007	20	21	32	10	25	35	81	28L, 28R | 1L, 1R	IAC	17.85	4.81	60	270	10	010	7.00	VCFG	Severe
SFO	07/16/2007	21	15	39	14	28	42	102	28L, 28R | 1L, 1R	IAC	17.42	6.75	60	270	10	007	9.00		None
SFO	07/16/2007	22	30	17	18	26	44	72	28L, 28R | 1L, 1R	IAC	18.77	6.39	60	270	10	007	9.00		None
SFO	07/16/2007	23	13	14	22	29	51	72	28L, 28R | 1L, 1R	IAC	20.36	7.56	60	280	10	007	9.00		None

Figure 10. ASPM Data for Runway Operations at KSFO, July 16, 2007

Table 1. Mean Nominal System Time (July 9, 2007)

Arrival Fix	Runway	Mean System Time (min)
BORED	KOAK29	12.0
SYNTH01	KOAK29	15.0
SYNTH03	KOAK29	10.8
LICKE	KSJC30	5.7
GROAN	KSFO28R	11.6
PYE	KSFO28L	14.6
SKUNK	KSFO28L	9.7
SKUNK	KSFO28R	10.1

Figure 11 through Figure 15 present System Time estimates as a function of time, for flights from the arrival fixes BORED, SYNTH01 and SYNTH03 to KOAK29. The blue line with circular markers in all of these figures depicts the nominal data for July 9, 2007, and the red line with the diamond-shaped markers depicts data for July 16, 2007 corresponding to a flow constrained situation. The marker positions depict the time of the day where a new measurement was made available to the Particle Filter, i.e., the System Time for a new flight was recorded and calculated from radar measurements. The mean System Time from July 9 data for these links was calculated to be 12.0 min, 15.0 min, and 10.8 min, respectively. Data from July 16 shows some deviation in mean System Time, especially between 10am and 12pm, and after 6pm. The increase in System Time for flights in arrival routes to KOAK may be due to the same reason as those expected for flights to KSFO. This aspect will be explored in greater detail when discussing the results for arrival routes to KSFO in the later figures. In general, when comparing the System Time estimates for July 16 with July 9, an increase of 6 min in the mean System Time was observed after 6 pm. The capacity of OAK, as shown in Figure 16, was 138 runway operations per hour for the nominal day. On July 16, the capacity went down to 110 after 7am. Note that very few flights arrived at OAK prior to 7am. Therefore, for the rest of the day, a lower capacity was observed at OAK on July 16, 2007.
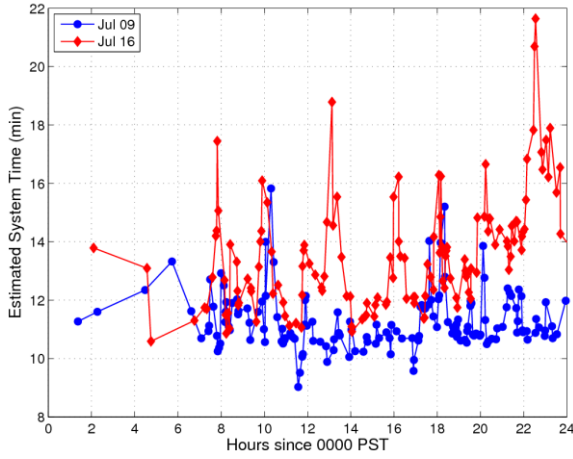
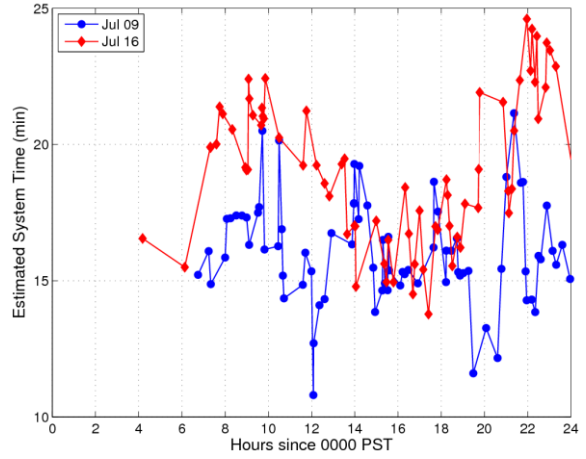**Figure 11. Evolution of System Time Estimate for BORED-KOAK29 Arrival Route**

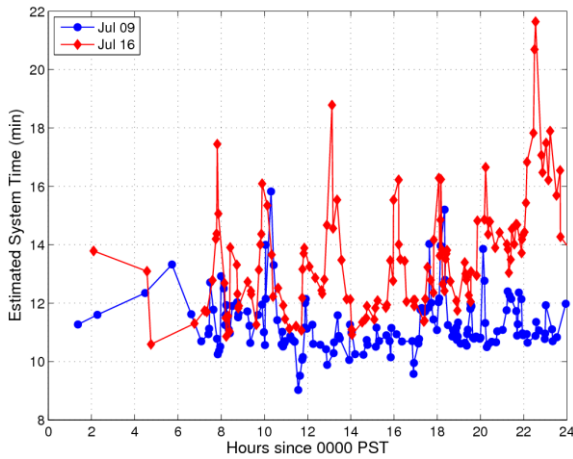**Figure 12. Evolution of System Time Estimate for SYNTH01-KOAK29 Arrival Route**

Figure 13. Evolution of System Time Estimate for BORED-KOAK29 Arrival Route
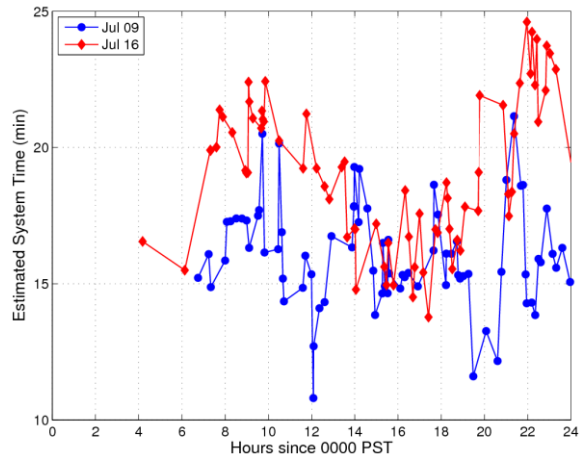

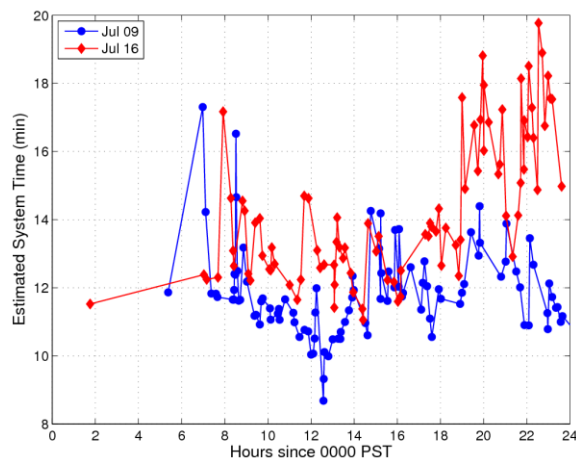**Figure 14. Evolution of System Time Estimate for SYNTH01-KOAK29 Arrival Route**

Figure 15. Evolution of System Time Estimate for SYNTH03-KOAK29 Arrival Route

American Institute of Aeronautics and Astronautics

Airport	Sched Dep Date	Local Hour	ADR+ Cap AAR	Sched Dep Date	Local Hour	ADR+ Cap AAR	Airport	Sched Dep Date	Local Hour	ADR+ Cap AAR	Sched Dep Date	Local Hour	ADR+ Cap AAR
OAK	07/9/2007	0	133	07/16/2007	0	138	SJC	07/9/2007	0	65	07/16/2007	0	65
OAK	07/9/2007	1	133	07/16/2007	1	138	SJC	07/9/2007	1	65	07/16/2007	1	65
OAK	07/9/2007	2	133	07/16/2007	2	138	SJC	07/9/2007	2	65	07/16/2007	2	65
OAK	07/9/2007	3	133	07/16/2007	3	138	SJC	07/9/2007	3	65	07/16/2007	3	65
OAK	07/9/2007	4	133	07/16/2007	4	138	SJC	07/9/2007	4	65	07/16/2007	4	65
OAK	07/9/2007	5	133	07/16/2007	5	138	SJC	07/9/2007	5	65	07/16/2007	5	65
OAK	07/9/2007	6	133	07/16/2007	6	138	SJC	07/9/2007	6	60	07/16/2007	6	65
OAK	07/9/2007	7	138	07/16/2007	7	110	SJC	07/9/2007	7	60	07/16/2007	7	65
OAK	07/9/2007	8	138	07/16/2007	8	110	SJC	07/9/2007	8	60	07/16/2007	8	65
OAK	07/9/2007	9	138	07/16/2007	9	110	SJC	07/9/2007	9	60	07/16/2007	9	65
OAK	07/9/2007	10	138	07/16/2007	10	110	SJC	07/9/2007	10	65	07/16/2007	10	65
OAK	07/9/2007	11	138	07/16/2007	11	110	SJC	07/9/2007	11	65	07/16/2007	11	65
OAK	07/9/2007	12	138	07/16/2007	12	110	SJC	07/9/2007	12	65	07/16/2007	12	65
OAK	07/9/2007	13	138	07/16/2007	13	110	SJC	07/9/2007	13	65	07/16/2007	13	65
OAK	07/9/2007	14	138	07/16/2007	14	110	SJC	07/9/2007	14	65	07/16/2007	14	65
OAK	07/9/2007	15	138	07/16/2007	15	110	SJC	07/9/2007	15	65	07/16/2007	15	65
OAK	07/9/2007	16	138	07/16/2007	16	110	SJC	07/9/2007	16	65	07/16/2007	16	65
OAK	07/9/2007	17	138	07/16/2007	17	110	SJC	07/9/2007	17	65	07/16/2007	17	65
OAK	07/9/2007	18	138	07/16/2007	18	110	SJC	07/9/2007	18	65	07/16/2007	18	65
OAK	07/9/2007	19	138	07/16/2007	19	110	SJC	07/9/2007	19	65	07/16/2007	19	65
OAK	07/9/2007	20	138	07/16/2007	20	110	SJC	07/9/2007	20	65	07/16/2007	20	65
OAK	07/9/2007	21	138	07/16/2007	21	110	SJC	07/9/2007	21	65	07/16/2007	21	65
OAK	07/9/2007	22	138	07/16/2007	22	110	SJC	07/9/2007	22	65	07/16/2007	22	65
OAK	07/9/2007	23	138	07/16/2007	23	110	SJC	07/9/2007	23	65	07/16/2007	23	65

Figure 16. ASPM Data for Runway Operations at KOAK and KSJC

Figure 17 shows the evolution of estimated System Time for the arrival route from LICKE to KSJC30. It may be observed that in general, the mean System Time obtained from data for both days are very close to each other. The nominal System Time on July 9 shows an increase between 6am and 9am. According to the ASPM report for KSJC, shown in Figure 16, airport capacity went down briefly from 65 to 60 runway operations per hour on July 9 in this time segment, although no weather impact was recorded. At all other times, including all of July 16, airport capacity remained at 65 runway operations per hour.

The evolution of System Time estimates for runways KSFO28L and KSFO28R are shown in Figure 18 through Figure 21. It should be observed that the decrease in airport capacity that was noted in Figure 10 does not necessarily affect System Time in all arrival routes. For example, as shown in Figure 18, PYE-KSFO28L does not appear to show any deviation in System Time. However, a significant deviation in System Time in any one arrival route may be sufficient to initiate TFM into the terminal area, since the effect will be more pronounced downstream where arriving streams of aircraft combine into one landing stream. It should be noted that even though Figure 19 shows that the arrival route SKUNK-KSFO28L shows no significant deviation in System Time, this may be misleading because on July 16, data shows that no flights from SKUNK landed on KSFO28L after 7pm, and instead, landed on KSFO28R given in Figure 20. Flights from SKUNK to KSFO28R, do exhibit an increase in System Time after 7pm, as shown in Figure 20.

Perhaps the most significant deviation in System Time is seen flights arriving from the fix GROAN, shown in Figure 21. It should be noted that an increase in System Time is observed between 8am and 10am even for the nominal data from radar measurements on July 9. However, as shown by the estimated System Time on July 16, the System Time continues to increase in this time interval, indicating variation in System Time. An increase in System Time is also seen after 7pm, for arrival routes to KSFO.

When compared with the ASPM data for KSFO, shown in Figure 9 and Figure 10, the increase in System Time between 9am and 12pm, and then again from 7pm to 10pm, are clearly reflected in the drop in airport capacity in these time periods.
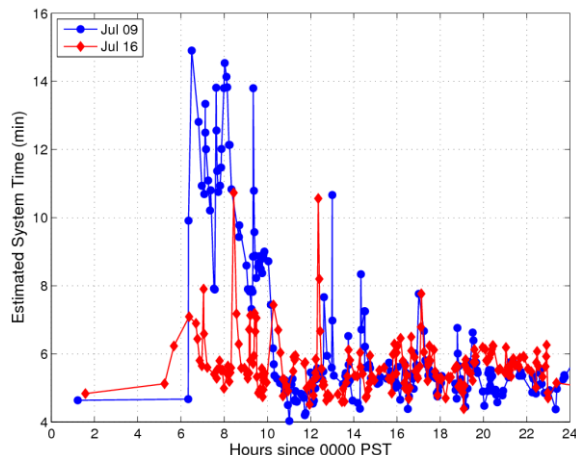

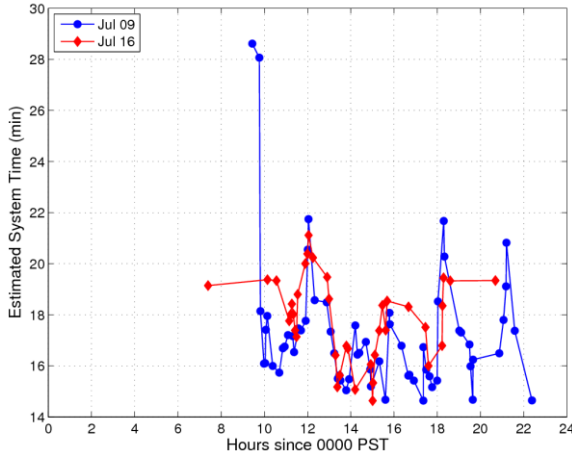**Figure 17. Evolution of System Time Estimate for LICKE-KSJC30 Arrival Route**

Figure 18. Evolution of System Time Estimate for PYE-KSFO28L Arrival Route
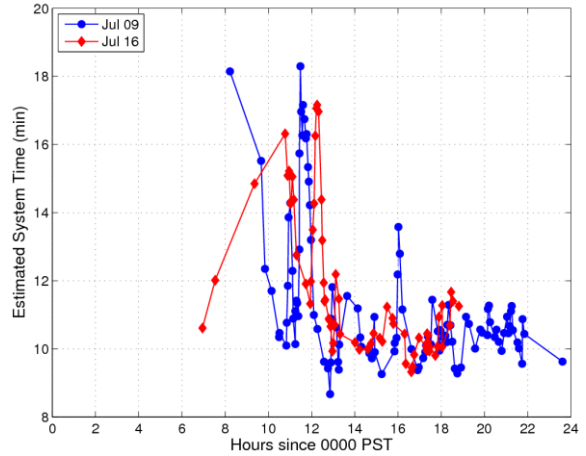

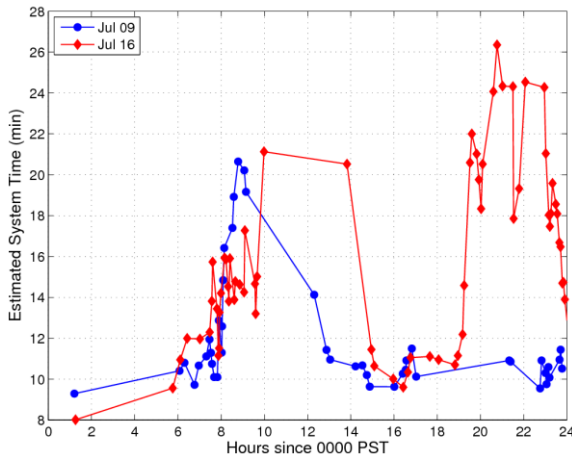**Figure 19. Evolution of System Time Estimate for SKUNK-KSFO28L Arrival Route**

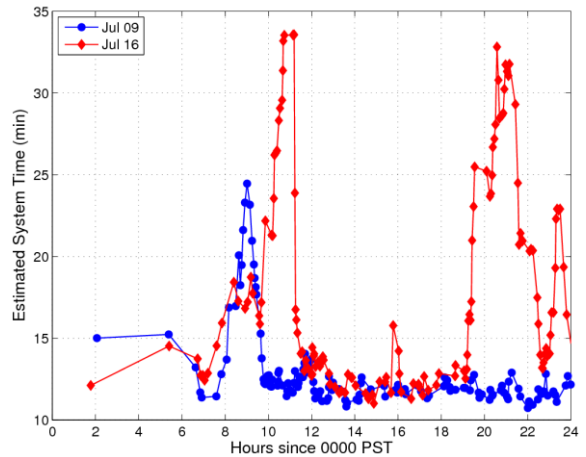**Figure 20. Evolution of System Time Estimate for SKUNK-KSFO28R Arrival Route**

Figure 21. Evolution of System Time Estimate for GROAN-KSFO28R Arrival Route

The results presented so far indicate the Particle Filter estimation algorithm is able to the employ historic data and the current measurements to reveal the dynamic behavior of the System Time. The deviations observed from the System Time estimator have been corroborated with independently obtained ASPM data. In particular, it has been shown that there is a strong link between the runway capacity of the airport being studied, and the System Time of arrival routes that lead to that airport. When the runway capacity decreases due to weather-related or other reasons in any time-segment, the System Time shows a corresponding increase in the same time segment.

Although only mean values of the System Time have been presented in this section, the Particle Filter is able to calculate its complete statistical distribution in the form of histograms. This histogram can be used to create a trigger for initiating TFM in the terminal area, as will be discussed in Section IV.

D. Computational Effort in the Particle Filter

Before closing this section, a few discussions about the computational effort involved in the Particle Filter implementation are in order. In the current implementation, the Particle algorithm was programmed using GNU C with the GNU Scientific Library[25] on a 2.8GHz 64bit dual-core processor. The execution time using 24-hour radar data was less than 1 min, with 10000 particles per arrival route. As noted before, there are approximately 18 routes, with approximately 220 flights per route. In the current implementation, the algorithm scales linearly with the number of arrival routes. This is because, each route is assumed to be an independent link from an arrival fix to a runway, and no merge or split of flows has been taken into account. Introduction of additional complexities in the

American Institute of Aeronautics and Astronautics

network topology may increase the computing time. However, computer systems employing modern Graphical Processing Units can be used to accommodate this increase in complexity[28].

IV.   Triggering TFM Initiatives based on Hypothesis Testing

Section III demonstrated the estimation of queuing network parameters using a Particle Filter. It was shown there that the Particle Filtering algorithm can estimate increase in the System Time arising from traffic congestion. This observed increase can be used to trigger traffic flow management algorithms. However, since these are statistical distributions, Statistical Decision Theory[9] must be employed to create actionable decisions. A method for triggering for Traffic Flow Management algorithms based on based on the Hypothesis Testing methodology[9] will be described in this section.

Hypothesis testing is used to establish the statistical significance of an event. The objective is to determine if the event occurred entirely due to chance or occurred due to a definite cause. In keeping with the formalism associated with Hypothesis Testing, it is necessary to define a *Null Hypothesis H_0*, and an *Alternative Hypothesis H_a*. Typically, the purpose of the Null Hypothesis is to establish that no relationship exists between two measured phenomena. The Alternative Hypothesis can either be a negation of the Null Hypothesis, or it can be used to measure the likelihood of an alternative to H_0 such as the second phenomena happened due the result of a different set of conditions. Once H_0 and H_a are suitably defined, a decision table as shown in Table 2 can be created. The response to H_0 can either be an acceptance or rejection of the hypothesis, followed by certain actions based on acceptance or rejection. The entries of the 2×2 decision table are then populated by the consequences of accepting or rejecting the hypothesis when either of the hypotheses is true.

Table 2. 2×2 Decision Table

	H_o	H_a
Accept H_o	No Decision Error	Type II Decision Error
Reject H_o	Type I Decision Error	No Decision Error

A. Hypothesis Testing Based on Statistical Decision Theory

In Table 2, accepting H_0 is equivalent to making a decision under the assumption that there is no relationship between two observed phenomena. Therefore, if H_0 is true, then its acceptance does not lead to a decision error. On the other hand, rejecting H_0 when it is true results in a decision error that is known as a *Type I Decision Error*. A converse analysis can be performed on the Alternative Hypothesis H_a. It should be noted that if H_a is defined as a negation of H_0, then the following is true:

$$H_0 \text{ is FALSE } \Longleftrightarrow H_a \text{ is TRUE} \tag{12}$$

However, in general, the implication can only be defined leftwards, because when H_0 is false, an untested alternative hypothesis $\bar{H}_a$ may be true without H_a being true. Therefore, if H_a is true, then rejecting H_0 and not making a decision based on H_0 also does not lead to error, because H_0 is false. However, accepting H_0 when H_a is true is a decision that may result in unintended consequences and will result in a *Type II Error*. In the following sections the Null and Alternative Hypotheses will be formulated in the context of Traffic Flow Management.

B. Definition of the Null Hypothesis in the Context of TFM

The Null Hypothesis and Alternative Hypothesis can be defined in order to frame the hypothesis testing methodology for triggering TFM:

H_0: There is no delay experienced in a flight's trajectory in a given route, and the observed deviation in System Time can be attributed to normally occurring statistical variations.

H_a: There is delay experienced and the observed deviation in System Time is due to actual causes.

In the above definitions, a deviation in System Time is measured by comparing the estimated System Time distributions with the System distribution for a normal day.

The acceptance of H_0 implies that no TFM action need to be taken. The rejection of H_0 implies that some TFM action is taken. In general, the decision to perform TFM depends on the confidence with which H_0 is rejected. Based

on these definitions, the 2×2 Decision Table given in Table 2 can be converted into a decision table more specific to TFM needs, as shown in Table 3.

Table 3. Decision Table for TFM

	No Delay	Delay
Do not Perform TFM	No Decision Error	Type II Decision Error
Perform TFM	Type I Decision Error	No Decision Error

This paper develops a method for calculating the likelihood of rejecting H_0. In other words, the likelihood that the deviation in System Time was not due to normally occurring statistical variations is evaluated. It should be noted that:

- Since the data for flight trajectories and their respective System Times corresponds to historic radar measurements, TFM action is already implicitly included in the System Times. Therefore, basing a decision on this data allows one to measure the probability of the occurrence of a Type I Decision Error.
- The probability of "No Decision Error" can be obtained from the complement of the probability of the Type I Decision Error.
- The scope of the present work does not extend to calculating the probability of a Type II Decision Error.

C. Comparison of System Time Distributions

As noted in the previous section, the decision to perform TFM is based on the confidence with which the Null Hypothesis can be rejected. This is equivalent to examining the confidence with which one can reject the notion that the estimated System Time distributions and a nominal "good" day, at the same time, are similar to each other. Alternatively, one may study the distribution of the Delay Time, which is given by the difference between the System Time distribution currently observed, and the System Time distribution in the same time-interval on the nominal day.

Since the Delay Time distribution is obtained by taking the difference of two independent distributions, the histogram of the Delay Time may be obtained by a convolution operation. Let the System Time distributions on the nominal day and current day be denoted by the discrete PDFs $P_1(t) = \{(p_{11}, T_1), (p_{12}, T_2), \dots, (p_{1n}, T_n)\}$ and $P_2(t) = \{(p_{21}, T_1), (p_{22}, T_2), \dots, (p_{2n}, T_n)\}$ respectively, where it is assumed that the time intervals $T_i = [t_{i-1}, t_i)$, over which both PDFs are defined are identical. Let τ_1 and τ_2 be sampled from $P_1(t)$ and $P_2(t)$, respectively. The delay, defined by Δ, is given by $\Delta = \tau_2 - \tau_1$. It follows that the distribution of Δ can be obtained by convolving the distribution of τ_2 and $-\tau_1$, where the distribution of $-\tau_1$ is given by $\bar{P}_1(t) = \{(p_{11}, \bar{T}_1), (p_{12}, \bar{T}_2), \dots, (p_{1n}, \bar{T}_n)\}$, where

$$\bar{T}_i = [-t_{n-i-1}, -t_{n-i})$$ (13)

Consequently, the Delay Time distribution is given by the discrete PDF $\Delta(t) = \{(\Delta_1, T'_1), (\Delta_2, T'_2), \dots, (\Delta_m, T'_m)\}$, where

$$m = 2n - 1$$

$$\Delta_i = \sum_{j=max(1, i+1-n)}^{min(i,n)} p_{1j} p_{2[i-j+1]}, \qquad i = 1, \dots, m$$

$$T'_i = [t'_{i-1}, t'_i), \qquad t'_i = t'_0 + (i-1)dt', \qquad i = 1, \dots, m$$

$$t'_0 = t_0 - t_n, \qquad dt' = \frac{(t_n - t_0)}{n-1}$$

(14)

In particular, if the mean and the variance of the two System Time distributions are (m_1, v_1), and (m_2, v_2), respectively, then the mean and variance of the Delay Time distribution is given by:

$$m_{Delay} = m_2 - m_1$$
$$v_{Delay} = v_2 + v_1$$ (15)

D. Assessing the Confidence in the Null Hypothesis by Evaluating a Test Statistic

Since a Delay Time distribution can be calculated using the two System Time distributions, the confidence with which one may reject the Null Hypothesis can be obtained by studying the distribution $\Delta(t)$, obtained by using Eq. (14). However, while the full distribution is available for analysis using the particle filter approach, statistical analysis limits hypothesis testing to the use of the first two moments, namely, the mean and the variance. To this end, the test statistic z_{obs} is defined as follows:

$$z_{obs} = \frac{m_{Delay}}{\left(\dfrac{\sqrt{v_{Delay}}}{\sqrt{N}}\right)} \tag{16}$$

where N is the number of observations used to obtain the distribution.

In the present problem, it is the number of flights in a given time interval over which the TFM trigger is studied. The term in the denominator of Eq. (16) is known as the standard error, and is a strong function of the number of samples. The test statistic z_{obs} can be interpreted as a random variable sampled from a distribution with zero-mean and unit-standard deviation.

If the Null Hypothesis H_0 is assumed true, then $m_{Delay} = 0$, and the natural variation is governed by v_{Delay}. The probability that a value $z \geq z_{obs}$ occurred in this distribution is known as the *p-value*. A low p-value indicates a low probability for the occurrence of $z \geq z_{obs}$ and the fact that a low probability event actually occurred is a sufficient condition for the rejection of the Null Hypothesis.

Consequently, for a p-value of α, one can be 100α per cent confident of accepting the Null Hypothesis, and conversely, one can be $100(1 - \alpha)$ per cent confident of rejecting the Null Hypothesis.

Under the assumption that the Delay Time distribution is Gaussian with unit standard deviation, the p-value α can be calculated from the CDF of the Gaussian distribution. It can be observed from Eq. (16) that the confidence with which H_0 can be rejected is dependent on the number of samples used to define the histogram. Since $z_{obs} \propto \sqrt{N}$, as N increases, the test statistic becomes larger for the same value of m_{Delay}, and α becomes exponentially smaller. Qualitatively, this implies that if a larger number of aircraft exhibit an increase in System Time from the nominal, one can place a greater confidence that TFM needs to be initiated.

It should be noted that the use of the Gaussian distribution is only accurate when the number of flights is large. Since the number of aircraft flying the arrival routes over a decision period of one to two hours is small, it is more appropriate to use Student's t-distribution. The t-distribution is a one-parameter distribution given by:

$$p(t) = \frac{\Gamma\left(\dfrac{\nu + 1}{2}\right)}{\sqrt{\nu\pi}\,\Gamma\left(\dfrac{\nu}{2}\right)}\left(1 + \frac{t^2}{\nu}\right)^{-\frac{\nu+1}{2}} \tag{17}$$

where the parameter ν is the number of degrees of freedom of the distribution, and is given by $\nu = N - 1$. As ν increases, the t-distribution approaches the Gaussian distribution with zero mean and unit standard deviation.

E. Results for Traffic Flow into San Francisco

The hypothesis testing methodology is demonstrated using radar data in the SFO terminal area for July 16, 2007. The nominal data is from radar measurements for July 9, 2007 and the Null Hypothesis is that an observed deviation in System Time at a given time on July 16 is due to naturally occurring variations in the System Time.

Section III illustrated the estimation of System Time using the Particle Filter algorithm. Figure 11 through Figure 21 presented the mean values of the System Time for the two days considered in this research. In addition to the time histories of the means, the hypothesis testing methodology requires instantaneous variances of the estimates. As discussed in Section III, Particle Filter algorithm allows the calculation of these from instantaneous histograms of the estimates.

The evolution of the histogram for arrival routes BORED-KOAK29, LICKE-KSJC30, and GROAN-KSFO28R, are shown in Figure 22, Figure 23 and Figure 24, respectively. In these figures, the blue histogram is used to represent the discrete PDF of System Time from the nominal data obtained from radar measurements for July 9, 2007. The magenta histogram is used to represent the discrete PDF of System Time for the current day observation, July 16, 2007. In all three figures, the discrete PDFs are calculated using bin sizes of 1-minute, and are superimposed on the mean value of the System Time estimated at that time step.

The observed variations in mean System Time have already been discussed in Section II. In this section, the computation of the confidence with which the Null Hypothesis can be rejected for the three arrival routes will be presented.
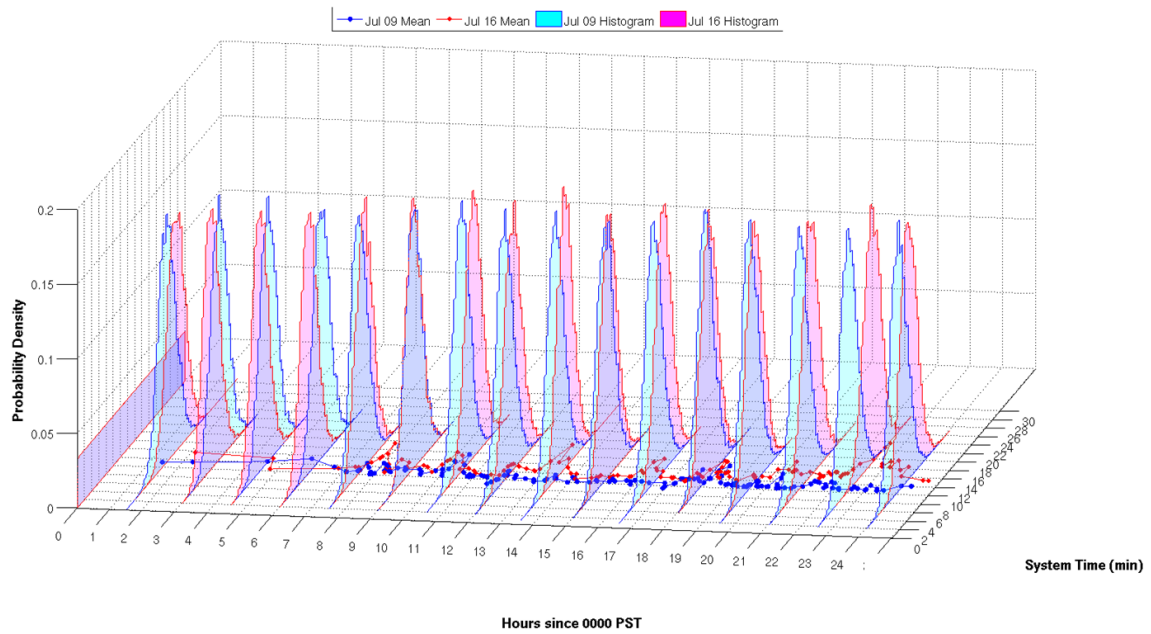
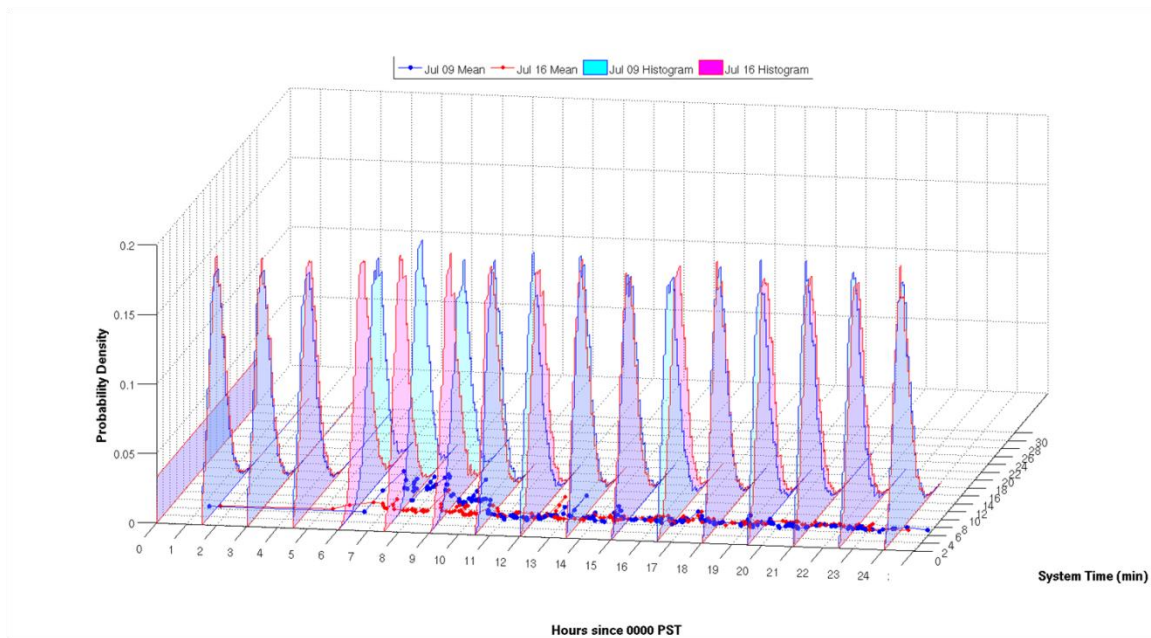**Figure 22. Evolution of System Time Probability Density Function, BORED-KOAK29**

Figure 23. Evolution of System Time Probability Density Function, LICKE-KSJC30
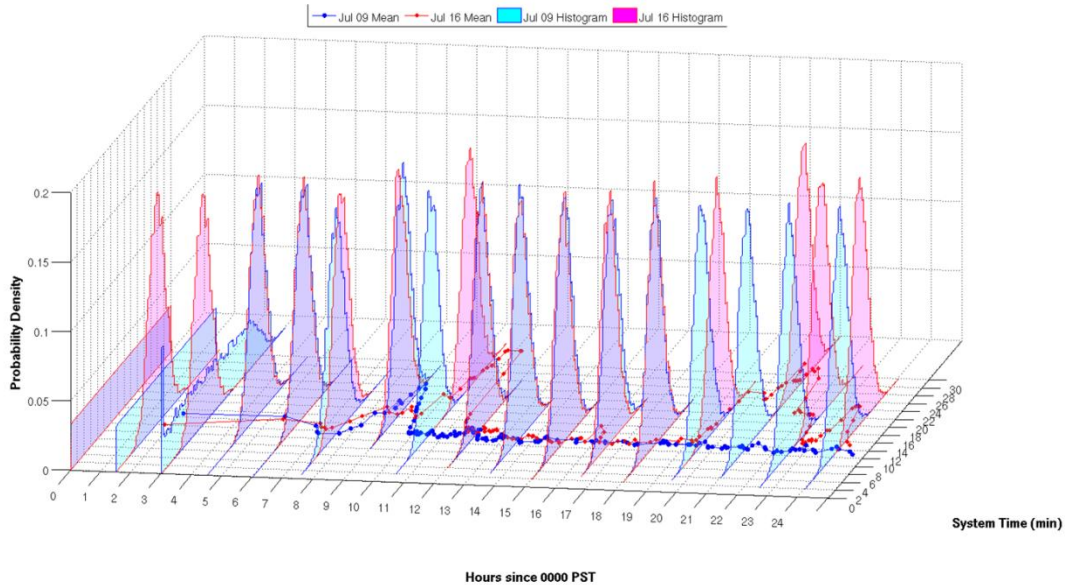
Figure 24. Evolution of System Time Probability Density Function, GROAN-KSFO28R

Figure 25 shows the confidence with which one can reject the notion that deviation in System Time was due to natural statistical variation, for the BORED-KOAK29 arrival route. Figure 26 and Figure 27 show similar plots for the LICKE-KSJC30 arrival route and GROAN-KSFO28R arrival route, respectively. In all figures, the minimum confidence is 50%, because values lower than this implies a confidence greater than 50% that the Null Hypothesis is true. In some cases, the confidence cannot be calculated, because the number of aircraft arriving in a given time segment is too low, or zero. Furthermore, calculation of confidence when the nominal mean System Time is greater than the current mean System Time is also not performed, because Delay Time is only defined when the current System Time is greater than the nominal System Time.

Figure 25 through Figure 27 should be compared with Figure 11, Figure 17, and Figure 21, respectively. Comparison of these figures reveals with how much confidence one can say that an observed delay was large enough to require TFM. For example, only in one instance in the LICKE-KSJC30 route can one have 75% confidence that delay was not due to natural statistical variation. For the rest of the day, the confidence of rejecting the Null Hypothesis is low. On the other hand, when comparing the current and nominal System Times for the BORED-KOAK29 arrival route with the confidence of rejecting H_0, one can conclude with a confidence of greater than 75% that TFM was required after 6 pm.

The confidence plot for the GROAN-KSFO28R, shown in Figure 24 shows two

Figure 25. Confidence that Delay is not due to Natural System Time Variation, BORED-KOAK29

segments where the confidence of rejecting H_0 is nearly 100%: between 10 am and 12 pm, and again, after 7 pm. Whenever the System Time variation is observed, it can be observed that System Time for both the nominal data and current data increase after 9 am, however, it is only after 10 am that the currently observed System Time is greater than the nominal System Time. Therefore the increase in System Time may be attributed to statistical variations due to other phenomena.
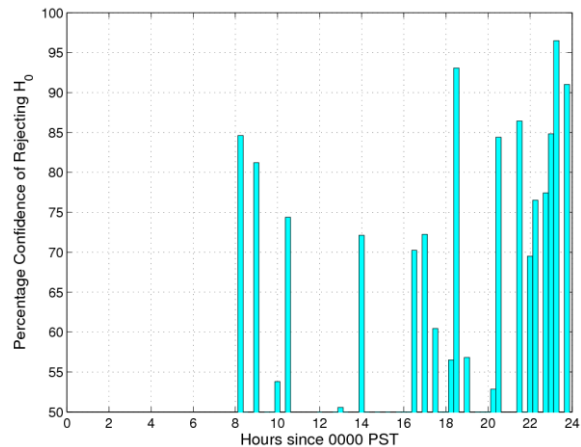
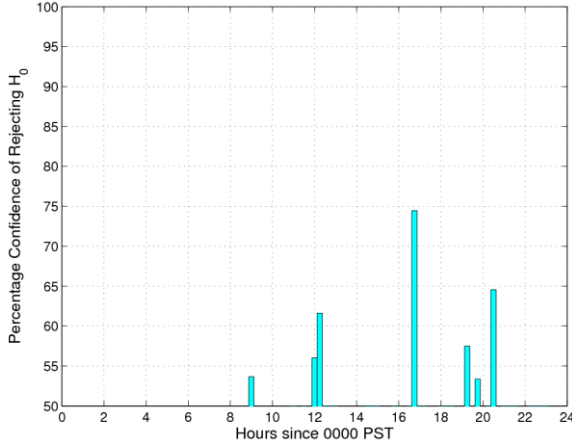American Institute of Aeronautics and Astronautics

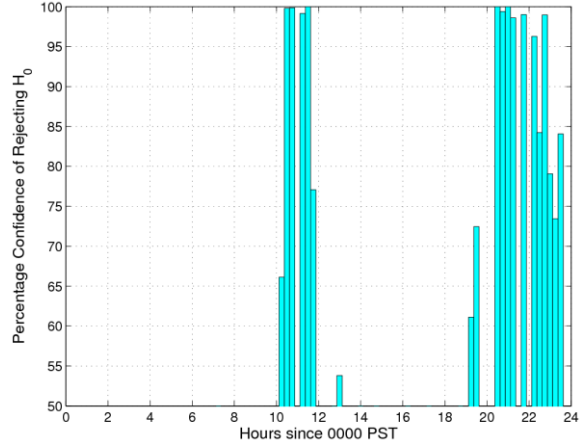**Figure 26. Confidence that Delay is not due to Natural System Time Variation, LICKE-KSJC30**

Figure 27. Confidence that Delay is not due to Natural System Time Variation, GROAN-KSFO28R

The statistical hypothesis testing methodology for triggering TFM algorithms developed in this section of the paper can be used in a variety of statistical decision making situations that commonly arise while dealing with real air traffic data. In the present example, the hypothesis testing based on Particle Filter estimated System Time clearly indicated the need for initiating TFM along two arrival routes into San Francisco. This methodology can be used to construct decision support tools to aid traffic managers arrive at TFM decisions in a more logical manner. Section V will demonstrate the use of the queuing network parameters estimated by the Particle Filter for optimizing stochastic traffic flows.

V.   Runway Load Balancing

The queuing network parameters estimated by the Particle Filter can be used address a variety of resource allocation problems that arise in air traffic flow control. Specifically, the estimated parameters can be used to formulate a variety of runway management problems. The formulation described in the prior sections can be used to examine a large class of problems that can arise in NASA's SORM program.

The runway load balancing problem can be defined as follows. Given n arrival fixes to m runways, the objective is to split the arrival flows at each fix, between the runways such that m flows of aircraft landing on the runways are in a desired ratio to each other. The analysis is applicable to time-varying flows, and also accounts for the fact that changes in the flow rate at the arrival fixes are felt at the runway only after a period of time. The formulation is stochastic in the sense that the split fractions are mean values.

A. Analytical Development

A schematic diagram of the 28L/28R runway load distribution problem at San Francisco is given in Figure 28. The flow rate of aircraft at the n arrival fixes are denoted by λ_{A_i}, $i = 1, \dots, n$. The flow rate of aircraft at the m runways are denoted by λ_{D_i}, $i = 1, \dots, m$.

San Francisco airport has 4 runways: KSFO01L, KSFO001R, KSFO28L, and KSFO28R, of which runways 01L and 01R are used mostly for departing flights. Runways 28L and 28R are used primarily for flights arriving into KSFO, although some departing flights also use these runways. The present research will be focused on runways 28L and 28R.

Five arrival fixes feed the traffic into the two runways: BONNS, GROAN, PIRAT, PYE, and SKUNK. For the purpose of present analysis, departing traffic from the terminal can be treated as an arrival fix; consequently, $n = 6$. The objective of the runway load balancing process is to direct traffic into the two runways from each of the arrival fixes and the departing traffic stream, so as to load the two runways at a certain flow rate. This process must explicitly recognize the fact the aircraft streams from different arrival fixes take different amounts of time to reach the runways. Moreover, these System Times are stochastic variables.
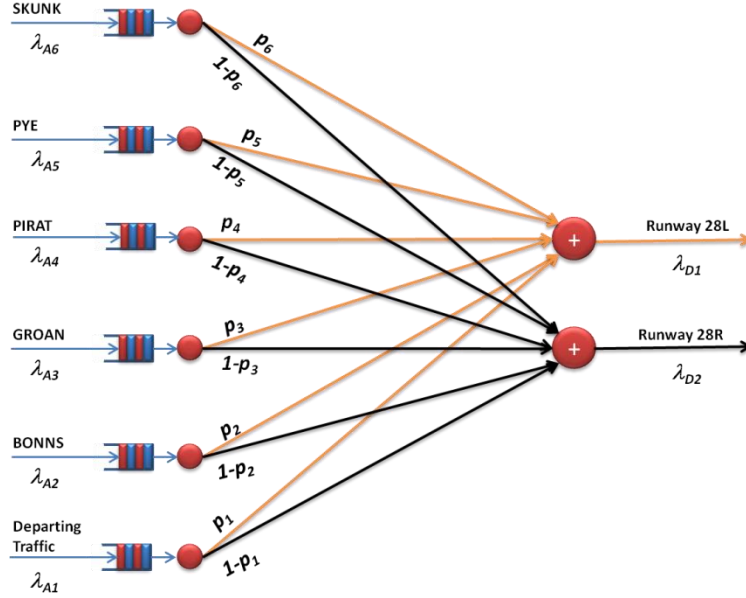
Figure 28. Schematic Diagram of the Distribution of Traffic Load between Runways at KSFO

Let T_{ij} be the time taken for a flight from the ith arrival fix to the jth runway. Note that these are the stochastic variables estimated by the Particle Filter described in Section III. If it is assumed that the runways are close to each other, then it can be assumed that $T_{ij} = T_i \ \forall j$. Furthermore, let p_{ij} be the fraction of the flow of arriving aircraft at the ith arrival fix that is directed towards the jth runway. The flow fractions p_{ij} are the *decision variables* in the current analysis, in the sense that their values at a given time t specify the fraction of traffic flow that are directed to each of the runways.

By virtue of the fact that $\sum_{j=1}^{m} p_{ij} = 1$, it can be assumed that

$$p_{im} = 1 - \sum_{j=1}^{m-1} p_{ij} \tag{18}$$

In the current work, using the formulation developed in this section, the flow rate of aircraft landing at runways 28L and 28R are given by the following two equations:

$$\lambda_{D_1}(t) = p_1(t - T_1) \cdot \lambda_{A_1}(t - T_1) + \cdots + p_6(t - T_6) \cdot \lambda_{A_6}(t - T_6)$$
$$\lambda_{D_2}(t) = [1 - p_1(t - T_1)] \cdot \lambda_{A_1}(t - T_1) + \cdots + [1 - p_6(t - T_6)] \cdot \lambda_{A_6}(t - T_6) \tag{19}$$

The total flow rate at the runways is given by $\lambda_D(t) = \lambda_{D_1}(t) + \lambda_{D_2}(t)$. From Eq. (19), it can be shown that:

$$\lambda_D(t) = \lambda_{A_1}(t - T_1) + \cdots + \lambda_{A_6}(t - T_6) \tag{20}$$

Let $p_{rwy}(t)$ be the desired fraction of the total flow landing on runway 28L, a time-varying quantity. Then the desired flow rates at the runways are given by $\lambda_{Des_1}(t)$ and $\lambda_{Des_2}(t)$, respectively, where

$$\lambda_{Des_1}(t) = p_{rwy}(t)\lambda_D(t)$$
$$\lambda_{Des_2}(t) = [1 - p_{rwy}(t)]\lambda_D(t) \tag{21}$$

To further simplify analysis, Eq. (19) can be studied at discrete time steps, where $t = k \cdot \Delta t$, and $T_i = s_i \Delta t$. Then the time argument in Eq. (19) and Eq. (21) can be identified by the time step k, and these equations may be rewritten as follows:

$$\lambda_{D_1}(k) = p_1(k - s_1) \cdot \lambda_{A_1}(k - s_1) + \cdots + p_6(k - s_6) \cdot \lambda_{A_6}(k - s_6)$$
$$\lambda_{D_2}(k) = [1 - p_1(k - s_1)] \cdot \lambda_{A_1}(k - s_1) + \cdots + [1 - p_6(k - s_6)] \cdot \lambda_{A_6}(k - s_6) \tag{22}$$

Using the above equations, the problem of runway load balancing requires one to find values of the decision variables $p_i(t)$ such that the flow rate at the runways $\lambda_{D_j}(t)$ are as close to the desired flow rates $\lambda_{Des_j}(t)$ in a Euclidian sense. This can be achieved by minimizing the difference between $\lambda_{D_j}(t)$ and $\lambda_{Des_j}(t)$ in a least-squares sense.

It should be noted that Eq. (19) is an under-determined system of linear equations and therefore there is no unique combination of the decision variables that will minimize the difference between the current and desired landing flow rates. The problem of runway load balancing at the kth time step, is thus posed as the following minimization problem:

$$\text{minimize } J = \frac{1}{2}(\lambda - \lambda_{Des})^\top Q(\lambda - \lambda_{Des}) + \frac{1}{2}(p - p_{Des})^\top R(p - p_{Des})$$
$$\lambda = \{\lambda_{D_1}(k) \ \lambda_{D_2}(k)\}^\top$$
$$\lambda_{Des} = \{\lambda_{Des_1}(k) \ \lambda_{Des_2}(k)\}^\top \tag{23}$$
$$p = \{p_1(k - s_1) \cdots p_6(k - s_6)\}^\top$$
$$Q, R > 0$$

In Eq. (23), p_{Des} is a vector of nominal values of the decision variables around which a solution to p is sought. In the present research, it is assumed that p_{Des} is a constant, i.e. $p_{Des} = p_{Des}\mathbf{1}$, although no significant advantage is gained by allowing p_{Des} to be a time-varying quantity. The matrices Q and R assign relative weights to the two components of the cost function J.

Equation (23) can be solved in a straightforward manner using a least-squares solution. For a TFM decision to have an effect at the kth time-step, the decision must be made at the $(k - s_i)$th step for the ith arrival fix, through the decision variable $p_i(k - s_i)$. Therefore, it may be assumed that $\lambda_{A_i}(k - s_i)$ is also known, and as a consequence, λ_{Des} is also known, using Eqs. (20) and (21).

The least-squares solution to Eq. (23) is obtained by setting $\partial J/\partial p$ to zero. This results in the following equation:

$$R(p - p_{Des}) + \Lambda^\top Q(\lambda - \lambda_{Des}) = 0 \tag{24}$$

where Λ is a matrix defined as follows:

$$\Lambda = \frac{\partial \lambda}{\partial p} = \begin{bmatrix} \lambda_{A_1}(k - s_1) & \cdots & \lambda_{A_6}(k - s_6) \\ -\lambda_{A_1}(k - s_1) & \cdots & -\lambda_{A_6}(k - s_6) \end{bmatrix} \tag{25}$$

Using Eqs. (20) and (22), and assuming that p_{Des} is a constant, it can be shown that:

$$\lambda_{D_1}(k) = [p_1(k - s_1) - p_{Des}]\lambda_{A_1}(k - s_1) + \cdots + [p_6(k - s_1) - p_{Des}]\lambda_{A_6}(k - s_1)$$
$$+ p_{Des}\lambda_D(k)$$
$$\lambda_{D_2}(k) = -[p_1(k - s_1) - p_{Des}]\lambda_{A_1}(k - s_1) - \cdots \tag{26}$$
$$- [p_6(k - s_1) - p_{Des}]\lambda_{A_6}(k - s_1) + (1 - p_{Des})\lambda_D(k)$$

In matrix notation, Eq. (26) can be rewritten as

$$\lambda = \Lambda(p - p_{Des}) + \lambda_0$$
$$\text{where, } \lambda_0 = \{p_{Des} \ (1 - p_{Des})\}^\top \lambda_D(k) \tag{27}$$

It should be noted that λ_0 is also a known vector. Using Eq. (27) in Eq. (24) results in the following expression for the control variables:

$$p - p_{Des} = (R + \Lambda^\top Q\Lambda)^{-1}\Lambda^\top(\lambda_{Des} - \lambda_0) \tag{28}$$

In Eq. (28), the matrix Λ has rank $(m - 1)$, and if a weight matrix R is not included, then a solution for p cannot be obtained. Secondly since p_i are flow fractions, the constraint $0 \leq p_i \leq 1$ must be satisfied at all times. If $p_{Des} = 0.5$, then to ensure that Eq. (28) provides a valid solution, one may check that the constraint $|p_i - p_{Des}| \leq 0.5$ is satisfied. If this constraint is not satisfied, then Eq. (28) can be solved with a matrix R' where $\|R'\| > \|R\|$ such that the constraint is satisfied.

B. Runway Flow Balancing Results for San Francisco

The runway load balancing methodology developed in the foregoing is next demonstrated using the radar data[19] for flights landing and taking off from KSFO runways 28L and 28R. July 9, 2007 data is used in the present study. Figure 29 shows the mean flow rate of aircraft over two-hour intervals on this day. Combined flows into runways 28L and 28R are given in this figure. The mean flow rates are periodic, and typically show two peaks, occurring in different segments of the day. This indicates that different arrival routes show increased traffic magnitude at different times, depending on the origin airports of the flights. For example, the PIRAT arrival fix is mostly used by air traffic from the Pacific.

Each set of histograms in Figure 29 corresponds to an arrival flow rate function $\lambda_{A_i}(t)$. The flow rate can be modeled as piecewise continuous functions. For the present research, these flows are modeled in two-hour segments. Note the present aggregation

Figure 29. Flow Rate of Aircraft from KSFO Terminals and Arrival Fixes

methodology will produce satisfactory results only if the number of aircraft in a time segment are sufficient to justify description using flow rates. It is further assumed that $\lambda_{A_i}(t)$ represents the mean flow rate of a stream of aircraft following a Poisson process, implying that the inter-arrival time of the aircraft can be modeled as an Exponential distribution.

Next, the traffic flow fractions into each of the runways from the arrival fixes are calculated to get an idea about the load distribution between runways. Figure 30 shows the fraction of flows from the arrival fixes and departure traffic to KSFO28L. The fraction of flows to KSFO28R can be obtained by subtracting these values from 1. The flow fraction is calculated by simply counting the number of flights that land at 28L from a given fix. Although the runways are situated close to each other, the destination runway is indicated in the radar data for the flight trajectory. In some cases, for a given segment of time, there may be no flights in an arrival route. The corresponding flow fraction then cannot be calculated. For example, there were no flights departing from 28L or 28R from the airport between 4am and 6am, and as a consequence, the data point in this figure is missing for the corresponding segment.
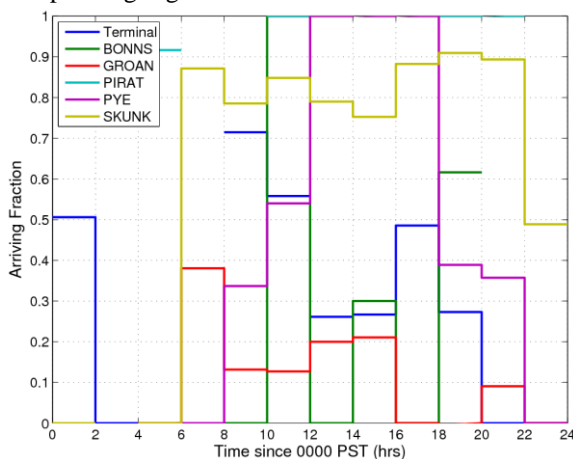

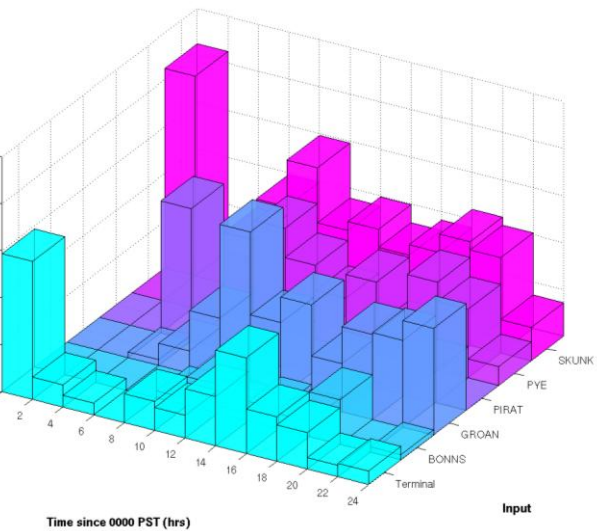**Figure 30. Observed Fraction of Traffic from Arrival Fixes to KSFO28L on July 9, 2007**
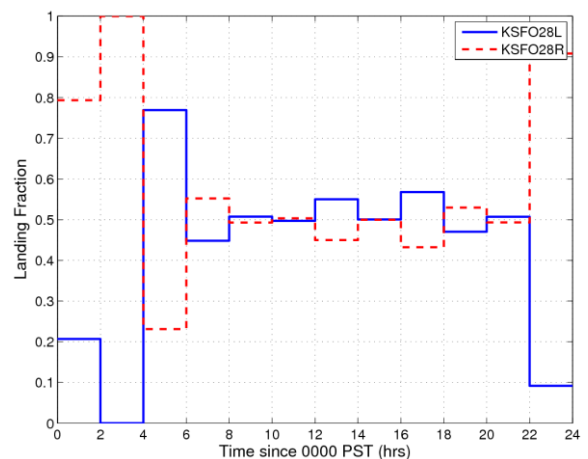

Figure 31. Observed Fractions of Traffic from Arrival Fixes to KSFO28L/28R on July 9, 2007

Based on the radar measurement data, the fraction of flows arriving at KSFO28L and KSFO28R from all arrival fixes for KSFO, as well as from the airport terminals, are shown in Figure 31. In this figure, the solid line

indicates the fraction of flows over two-hour intervals for 28L, and the broken line indicates the fraction for 28R. Note that they sum to unity. It may be observed that between 6 am to 10 pm, flows to the two runways are split approximately equally. However, at night, the data reveals that 28R is used preferentially. This may be due to a several reasons. For instance, San Francisco handles a large volume of international traffic involving heavy aircraft at night, requiring the use of the longer runway 28R.

Note that if the fleet mix in the arriving flow in a time interval is known, this can be incorporated in the formulation of the runway load balancing problem. For example, the flow from the ith fix to runway 28L is given by $p_i(t)\lambda_{A_i}(t)$. If the flow of aircraft arriving at the ith fix is composed of 3 different classes of aircraft that have fleet mix fractions of $p_{mix_1} + p_{mix_2} + p_{mix_3} = 1$, then three decision variables are available, one for each component of the fleet mix, and the analysis developed in the previous section can be used to obtain the fraction of flows of each component of the fleet mix. However, this level of detail was not pursued in the interest of brevity.
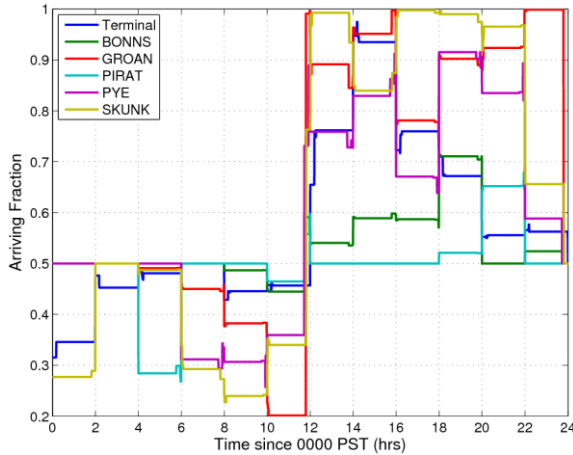

Figure 32. Fraction of Arriving Flows from Fixes to KSFO28L Derived by the Optimal Runway Flow Balancing Algorithm
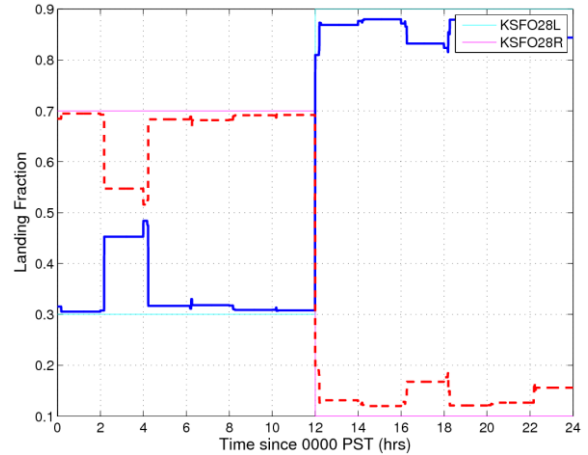

Figure 33. Fraction of Arriving Flows from Fixes to KSFO28L and KSFO28R Derived by the Flow Balancing Algorithm

Next, the flow balancing methodology is applied to the traffic flows. The flow fractions resulting from these computations are given in Figure 32. In this example, the runway load balancing requirements are specified as follows: during the first half of the day, it is desired to split the flows 30%-70% between runways 28L and 28R. For the second half of the day, a 90%-10% split is desired. Note that these are contrived objectives to illustrate the methodology. The nominal values of the flow fractions are $p_{des} = 0.5$; therefore, the variations in the flow fraction values over each two-hour time period, start with a value of 0.5. The algorithm chooses the appropriate value that will keep the flow fractions within the constraint $0 \le p_i(t) \le 1$. The mean System Time T_i for each arrival route is obtained using the Particle Filter algorithm on data for July 9, 2007. The mean System Time values for departing flights from the gates are assumed to be zero in the present study, due to the proximity of the runways to the gates. A more sophisticated study may include the taxi time for departing flights, so as to push back the aircraft from the gates, just in time to utilize the runways.

Figure 33 shows the flow fractions to the runways derived by the optimal flow balancing algorithm together with their desired values. It may be observed that except for the two-hour segment between 2 am and 4 am, the algorithm is able to maintain the landing flow fraction close to the desired values. In the 2 am-4 am segment, the net flow rate of aircraft arriving from the arrival fixes and terminal is a quite small. Consequently, a large change in landing flow fraction causes a very small change in the actual flow rate.

The temporal evolution of arrival and landing flow rates that are given in Figure 32 and Figure 33, show two types of variations. The first is the variation in the mean flow rates of aircraft arriving at the fixes. The second variation is a spike seen at the transition between time segments due to the different values of System Time for each arrival route, exhibited as time delays in the propagation equations.

The analysis and the results presented in this section show that stochastic optimization techniques coupled with advanced estimation algorithms based on queuing network formalism can be used to derive actionable decisions. The approach is general enough to be employed for the solution of flow control problems arising in runway utilization.

With minor modifications, the methodology discussed here can be used to balance traffic load between arrival fixes, and between arrival runways to achieve gate balancing. Moreover, this methodology can be tailored to optimize traffic flows on the taxiways and runways to achieve specific traffic objectives..

VI. Conclusions

This paper presented the feasibility of estimating traffic flow parameters from actual measurements, and employing methods from statistical decision theory to create actionable decisions. The proposed methodology uses queuing network representation to capture the traffic flow characteristics using a few statistical parameters. These queuing network parameters are then estimated using a Particle Filter. Since the parameters in the queuing network are described by non-Gaussian distributions, conventional estimation methods are not applicable. Using the actual radar track data for the San Francisco terminal area, it was shown that the Particle Filter can provide accurate queuing network parameter estimates under varying traffic conditions with modest computational resources. Specifically, the estimation of System Time from the radar track data for July 9, 2007 and July 16, 2007 was demonstrated to show that the Particle Filter accurately determined the increases in System Time due to reduction runway capacity.

Next, Statistical Decision Theory was used to formulate a decision support system for triggering traffic flow management in the terminal area. The approach is based on Hypothesis Testing for the statistical significance of observed delays. The algorithm continuously computes the confidence level in rejecting the null hypothesis that the changes in the System Time are due to normal statistical variation expected on a normal day. Whenever the confidence level in rejecting the null hypothesis goes above 75%, the algorithm triggers a TFM alert. This alert can be used to invoke flow controls into the terminal area, either through miles/time-in-trail or through Ground Delay Programs. The performance of the system was demonstrated by comparing the System Time estimates on July 9, 2007 with those on July 16, 2007. July 16 was a day in which the San Francisco airport experienced runway capacity reductions. The technique was able to distinguish between deviations in the System Time due to normal statistical variation and those due to actual capacity reducing events in the system.

As a second example, the System Time estimates were used to formulate an optimal runway load balancing methodology. In this approach, flow fractions are determined for traffic from arrival fixes so that the traffic at the runways will have a desired distribution. Complexity of this task arises from the different stochastic System Times experienced by traffic streams from the arrival fixes to the runways. The problem may be conceptualized as a flow synchronization problem to achieve a certain traffic load at the runways. The proposed approach is based on the Least Squares methodology, and its performance was demonstrated using radar track data from the San Francisco terminal area.

Acknowledgments

References

[1]Grabbe, S. R., and Sridhar, B., "Integrated Traffic Flow Management Decision Making," *AIAA Guidance, Navigation, and Control Conference*, Chicago, IL, Paper AIAA-2009-6008, Aug. 10-13, 2009.

[2]Sun, D., Sridhar, B., and Grabbe. S. R., "Traffic Flow Management Using Aggregate Flow Models and the Development of Disaggregation Methods," *AIAA Guidance, Navigation, and Control Conference*, Chicago, IL, Paper AIAA-2009-6007, Aug. 10-13, 2009.

[3]Grabbe, S. R., Sridhar, B., and Mukherjee. A., "Sequential Traffic Flow Optimization with Tactical Flight Control Heuristics," *Journal of Guidance, Control, and Dynamics*, Vol.32, No.3, pp 810-820, May-Jun. 2009.

[4]Grabbe, S. R., and Sridhar, B., "Congestion Management with an Aggregate Flow Model," *AIAA Guidance, Navigation, and Control Conference and Exhibit*, San Francisco, CA, Paper AIAA-2005-6277, Aug. 15-18, 2005.

[5]Rios, J., and Lohn, J., "A Comparison of Optimization Approaches for Nationwide Traffic Flow Management," *AIAA Guidance, Navigation, and Control Conference*, Chicago, IL, Paper AIAA-2009-6010, Aug. 10-13, 2009.

[6]Rios, J., and Ross, K., "Massively Parallel Dantzig-Wolfe Decomposition Applied to Traffic Flow Scheduling," *AIAA Guidance, Navigation, and Control Conference*, Chicago, IL, Paper AIAA-2009-6009, Aug. 10-13, 2009.

[7]Rios, J., and Ross, K., "Parallelization of the Traffic Flow Management Problem," *AIAA Guidance, Navigation and Control Conference and Exhibit*, Honolulu, HI, Paper AIAA-2008-6519, Aug. 18-21, 2008.

[8]Rios, J., and Ross, K., "Solving High Fidelity, Large-Scale Traffic Flow Management Problems in Reduced Time," *8th AIAA ATIO Conference*, Anchorage, AK, Paper AIAA 2008-8910, Sep. 14-19, 2008.

[9]Berger, J. O., *Statistical Decision Theory and Bayesian Analysis*, Springer-Verlag, New York, NY, 1985.

[10]Cassandras, C. G., and Lafortune, S., *Introduction to Discrete Event Systems*, Kluwer Academic Publishers, Boston, MA, 1999.

[11]Saaty, T. L., *Elements of Queuing Theory with Applications*, Dover Publications, New York, NY, 1983.

[12]Bertsimas, D., "An Exact FCFS Waiting Time Analysis for a General Class of G/G/s Queuing Systems," *Queuing Systems*, Vol. 3, No. 4, December 1988, pp. 305−320.

[13]Bertsimas, D., "An Analytic Approach to a General Class of G/G/s Queuing Systems," *Operations Research*, Vol. 38, No. 1, Jan.-Feb. 1990, pp. 139−155.

[14]Menon, P. K., Tandale, M. D., Kim, J., Sengupta, P., Kwan, J. S., Palaniappan, K., Cheng, V. H. L., Subbarao, K., Rosenberger, J., "Multi-Resolution Queuing Models for Analyzing the Impact of Trajectory Uncertainty and Precision on NGATS Flow Efficiency," Report No. OSS-0704-01 submitted under NASA Contract No. NNA07BC55C, November 2008.

[15]Tandale, M. D., Menon, P. K., Cheng, V. H. L., Rosenberger, J., and Thipphavong, J., "Queueing Network Models of the National Airspace System," *8th AIAA Aviation Technology, Integration, and Operations (ATIO) Conference*, Anchorage, AK, Paper AIAA-2008-8942, Sep. 14-19, 2008.

[16]Kim, J., Palaniappan, K., Menon, P. K., Subbarao, K., and Thipphavong, J., "Trajectory Uncertainty Modeling for Queueing Analysis of the National Airspace System," *8th AIAA Aviation Technology, Integration, and Operations (ATIO) Conference*, Anchorage, AK, Paper 2008-8854, Sep. 14-19, 2008.

[17]Menon, P. K., Tandale, M. D., Kim, J., Sengupta, P., Kwan, J. S., Palaniappan, K., Cheng, V. H. L., Subbarao, K., Rosenberger, J., "Efforts to Validate Multi-Resolution Queuing Models," Report No. OSS-0704-02 submitted under NASA Contract No. NNA07BC55C, Optimal Synthesis Inc., Los Altos, CA, July 2009.

[18]Menon, P. K., Tandale, M. D., Kim, J., Sengupta, P., "A Framework for Stochastic Air Traffic Flow Modeling and Analysis," *2010 AIAA Guidance, Navigation and Control Conference*, Toronto, Canada, Aug. 2-5, 2010.

[19]July 2007 Data recorded by the FAA Automated Radar Terminal System (ARTS), Provided by: San Francisco International Airport, Noise Abatement Office, Apr. 7, 2010.

[20]Thrun, S., Burgard, W. and Fox, D., *Probabilistic Robotics*, The MIT Press, Cambridge, MA, 2005.

[21]Gelb, A. (Editor), *Applied Optimal Estimation*, MIT Press, Cambridge, MA, 1989.

[22]Ristic, B., Arulampalam, S., and Gordon, N., *Beyond Kalman Filter*, Artech House, Boston, MA, 2004.

[23]Arulampalam, M. S., Maskell, S., Gordon, N. and Clapp, T., "A Tutorial on Particle Filters for Online Nonlinear/Non-Gaussian Bayesian Tracking," *IEEE Transactions on Signal Processing*, Vol. 50, No. 2, pp. 174-188, 2002.

[24]San Francisco International Airport Press Release, http://www.flysfo.com/web/page/about/news/pressres/, Accessed January 17, 2011.

[25]Galassi, M., Davies, J. Thieler, J., Gough, B., Jungman, G., Alken, P., Booth, M., and Rossi, F.., "GNU Scientific Library Reference Manual," *Network Theory Ltd.*, 3rd Edition, 2009.

[26]http://www.gnu.org/software/gsl/manual/html_node/The-Gamma-Distribution.html, July 21, 2010.

[27]http://aspm.faa.gov/, Jul. 15, 2010.

[28]Menon, P. K., Tandale, M. D., Wiraatmadja, S., and Lin, W.-M., "Computational Appliance for Rapid Prediction of Aircraft Trajectories (CARPAT)," Final Report Submitted under NASA Phase II SBIR Contract No. NNX08CA02C, Optimal Synthesis Inc., Los Altos, CA, February 2010.

American Institute of Aeronautics and Astronautics